View metadata, citation and similar papers at core.ac.uk
brought to you by CORE
provided by Institute of Volcanology and Seismology FEB RAS Repository

ISSN 0742-0463, Journal of Volcanology and Seismology, 2011, Vol. 5, No. 5, pp. 312–334. © Pleiades Publishing, Ltd., 2011.
Original Russian Text © A.V. Koloskov, G.B. Flerov, A.B. Perepelov, I.V. Melekestsev, M.Yu. Puzankov, T.M. Filosofova, 2011, published in Vulkanologiya i Seismologiya, 2011, No. 5, pp. 17–41.

Evolution Stages and Petrology of the Kekuknai Volcanic Massif as Reflecting the Magmatism in Backarc Zone of Kuril–Kamchatka Island Arc System. Part 1. Geological Position and Geochemistry of Volcanic Rocks

A. V. Koloskov[a], G. B. Flerov[a], A. B. Perepelov[b], I. V. Melekestsev[a], M. Yu. Puzankov[a], and T. M. Filosofova[a]

[a] *Institute of Volcanology and Seismology, Far East Branch, Russian Academy of Sciences, Piipa boulevard, 9, Petropavlovsk-Kamchatskii, 683006 Russia*
e-mail: kolosav@kscnet.ru

[b] *A. P. Vinogradov Institute of Geochemistry, Siberian Branch, Russian Academy of Sciences, ul. Favorskogo, 1A, Irkutsk, 664033 Russia*
e-mail: region@igc.irk.ru

Received October 25, 2010

Abstract—The evolution of the Quaternary Kekuknai volcanic massif (the western flank of the Sredinnyi Range in Kamchatka) has been subdivided into five stages: (1) the pre-caldera trachybasalt– basaltic andesite, (2) the extrusive trachyandesite–trachydacite, (3) the early trachybasalt, (4) the middle hawaiite–mugearite (with occasional occurrences of basaltic andesites), and (5) the late trachybasalt–hawaiite–mugearite (with occasional andesites) of areal volcanism. On the basis of petrologic data we identified the island arc and the intraplate geochemical types of rocks in the massif. The leading part in petrogenesis was played by dynamics of the fluid phase with a subordinated role of fractional crystallization and hybridism. Successive saturation of rocks with the fluid phase in the course of melt evolution stopped at the time of caldera generation when most fluid mobile elements and silica had been extracted. The geological and petrologic data attest to the formation of the massif in the environment of a backarc volcanic basin during the beginning of rifting with active participation of mantle plume components.

DOI: 10.1134/S074204631104004X

INTRODUCTION

The backarc volcanic basin of western Kamchatka is believed to originate in the Eocene in the area of an earlier marginal sea basin that occupied the location of the present-day "Okhotia." It was accompanied by crustal extension and emplacement of a set of parallel alkaline basalt dikes [Perepelov et al., 2007a]. Magmatic events also repeatedly occurred later. For example, in the area of western Kamchatka, in the Mt. Khukhch locality [Perepelov, et al., 2007b] these authors discovered Neogene K–Na alkaline magmas as a subvolcanic body of basanites of the "intraplate geochemical type," which is an indicator of volcanic activity in intracontinental rift settings. However, there is no general opinion on the problems of geodynamics and petrogenesis of the Late Cenozoic volcanic rocks for western Kamchatka. Some workers prefer subduction processes involving various mantle sources and addition of a fluid component from the underthrusting oceanic plate [Churikova et al., 2001; Volynets et al., 2010]. Others believe that subduction of the Kula oceanic plate under the Kamchatka continental margin terminated during Oligocene–Early Miocene time, and since then the volcanism in its backarc zone should be related to rifting [Perepelov et al., 2007b].

Overall, the occurrences of Late Cenozoic volcanism in western Kamchatka (large basalt plateaus, shield volcanoes in combination with structures of areal type) typically produce huge volumes of material erupted for rather short periods of time and may be likened to the provinces of "backarc trapp" or plateau basalts that are widely present in back-arc environments of Northern and Southern America. The origin of these provinces is considered within the framework of lithosphere extension models associated with backarc spreading [Hart, Carlson, 1987], or as a result of rifting above an anomalously hot mantle [White, McKenzie, 1989]. It is from this viewpoint that we shall consider features of geological setting and material composition of the Kekuknai volcanic area, one of the youngest and relatively well-preserved localities of magmatism in western Kamchatka.

At the same time, the Late Cenozoic backarc volcanism of the region under consideration in many

respects inherits peculiarities of composition that are typical of the preceding island arc volcanism. The intraplate characteristics in this are combined with subduction features [Volynets et al., 1995; Koloskov, 2006; Perepelov et al., 2007a, b]. Thus, we face the identification problem of a volcanic series, which is especially acute at a spatial or temporal boundary where the convergence of features is the most common.

Volcanic activity within large long-lived centers in the Sredinnyi Range is peculiar for the presence of calderas. They are not as large as those in eastern Kamchatka [Grib et al., 2003, 2009; Bindeman et al., 2010], but nonetheless occur in many volcanic massifs: Uksichanskii [Antipin et al., 1987; Volcanoes..., 1972; Martynov, Antipin, 2009], Ichinskii [*Vulkany* ..., 1972] and others. Caldera generation marks an important stage in the evolution of such a center. The generation of a caldera usually completes the formation of a shield edifice followed by the stage of multivent areal volcanism. In spite of the importance of this transitional period, the caldera generation mechanism itself was not practically considered in a general model of petrologic evolution for a concrete volcanic massif.

To deal with all these problems we require a careful analysis of the isotope–geochemical characteristics of volcanic rocks and extensive comparisons with "reference objects." Long-evolved and well-studied volcanic centers can be especially helpful. A good example of such an object is the backarc part of Kamchatka's Sredinnyi Range discussed in this paper.

GEOLOGICAL STRUCTURE AND THE LEVEL OF KNOWLEDGE OF THE REGION

The Kekuknai volcanic massif is the northeastern part of a large (66 × 30 km) complex volcanic edifice, which, in addition to Kekuknai Volcano (otherwise called Leningradets, 1401.2 m high), includes two other objects, the Bol'shoi (height 1299.9 m, western part) and Kunyru (height 1159.9 m, southern part) massifs with a total area of about 1400 km^2 and a rock volume of about 400–500 km^3. Together with the Bol'shaya Ketepana and Ichinskii massifs situated to NNE and SSW of this edifice they form a chain of major volcanic areals extending for 210 km along the western and northwestern spurs of Kamchatka's Sredinnyi Range at a great distance (about 400 km) from the Kuril–Kamchatka trench.

The above volcanic massifs are not, in spite of similar structural positions and closeness in origin time (supposedly about 1.5–2 Ma) and primary morphology in the form of shield-like volcanoes, similar in present-day morphology, formation stages, or their setting and composition of rocks. The Bol'shaya Ketepana volcanic massif has been less altered since then: it was severely destroyed by tectonic and denudation processes, including multistage glacial activity, but has preserved the characteristic features of a large shield volcano (base area is 630 km^2 and the ejected material volume is 185 km^3); its rock composition varies from basalts to andesites of high alkalinity [*Vulkany* ..., 1972]. In contrast, the Kekuknai and Ichinskii volcanic massifs have undergone significant changes, because their history contained several stages separated by long time intervals. Each stage of formation of these massifs involved different-scale endogenous processes and its own set and composition of effusive rocks. During periods between those stages the integrity of the fluid–magmatic system was violated, the previous edifices were intensely destroyed, and during each of the later stages their preserved fragments were partly or completely buried under newly ejected products.

The volcanic edifice of the Kekuknai massif is very complex in morphology and in its development history. The first published map of the area [*Vulkany* ..., 1972] shows shield edifices of the Bol'shoi and Kekuknai volcanoes, some non-differentiated lava covers, superimposed Holocene cinder cones, and their lava flows. The age of Kekuknai Volcano was determined as Middle Quaternary.

Extensive data on the geological structure of the region was obtained from a geological survey at a scale of 1 : 200000 [*Ob"yasnitel'naya* ..., 1986, 1992]. Based on these data, Early Quaternary, Late Quaternary, and recent volcanic rocks were recognized within the Kekuknai massif.

In summer of 2005 the authors of this paper carried out field works in the central part of the massif (Lake Bol'shoe Gol'tsovoe, Mount Chernaya, Dol Geologov). The study of collections of rock samples gave extensive analytic material on which this paper is based. The results of our analytical work are extensive, so the paper consists of two parts. The first part (this paper) presents a geological description of the Kekuknai massif and the results of petrologic and geochemical studies. The second part describes the mineralogical composition of the massif's rocks and develops a general geological–petrologic model.

Based on our studies, using the geological mapping data and available age datings, the geological structure of the Kekuknai massif can be described as follows (Fig. 1).

The massif's basement consists of tufaceous sedimentary rocks of the Middle Miocene Il'inskaya Formation rocks exposed in the massif's northern periphery, as well as the Early Miocene Viventekskaya and Kuluvenskaya formations of similar composition outcropping to SW of the area under consideration [*Ob"yasnitel'naya* ..., 1986] and in the SW part of the massif (Fig. 1).

The oldest part of the massif is the large shield-like Kekuknai Volcano, which supposedly formed during Late Pliocene–Early Pleistocene time. In the western sector of the edifice, in the side of the caldera, a 491-m-thick representative section is described in great detail [*Ob"yasnitel'naya* ..., 1986]. The section consists of alternating flows of olivine–clinopyroxene (with or

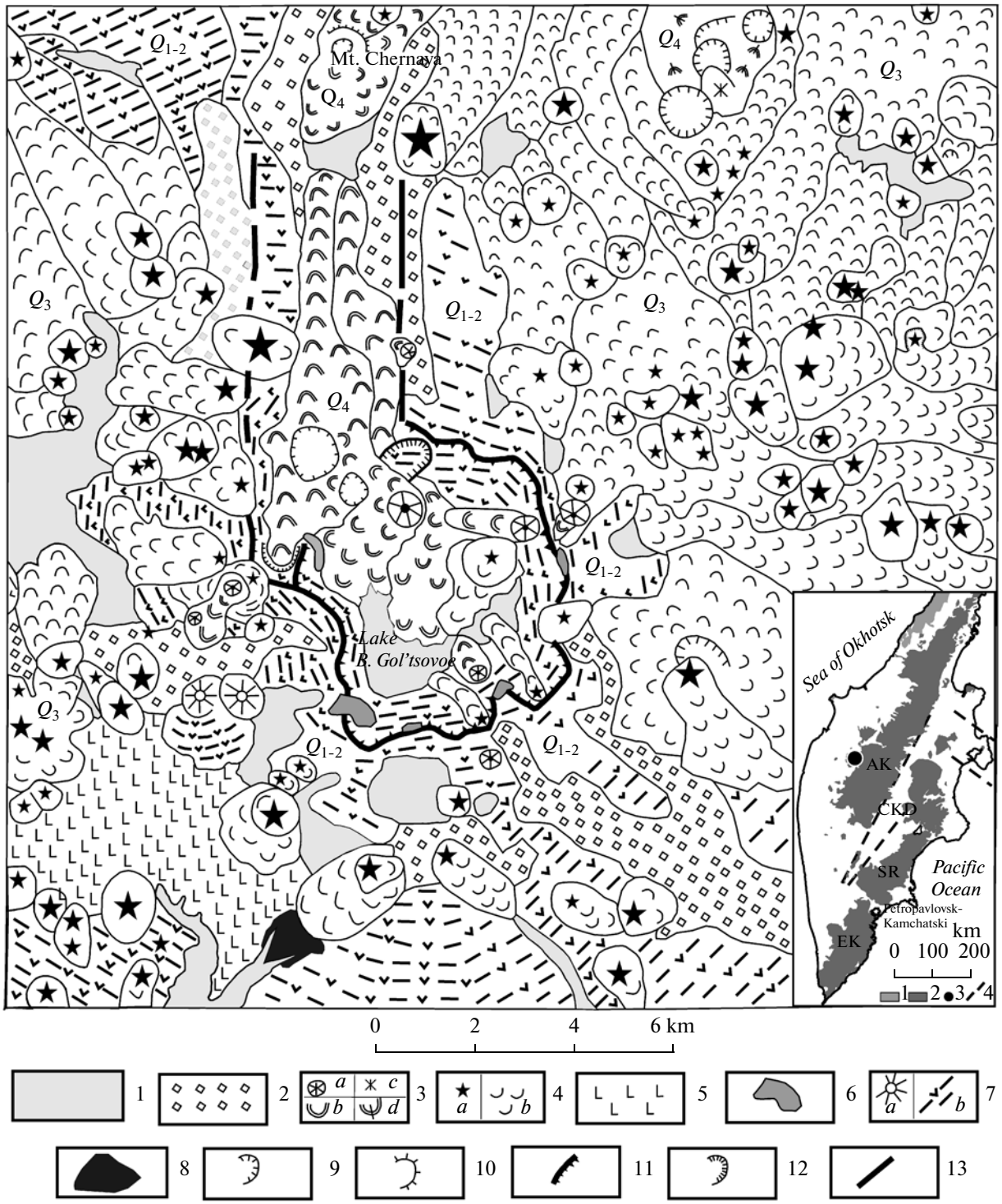

without plagioclase subpenocrysts and with accompanying magnetite) trachybasalts, plagioclase–bipyroxene (with olivine and amphibole or without them) trachyandesite basalts and basaltic andesites and horizons of tuffs and tuff breccias of the same composition. The later pre-caldera stage of the volcano evolution is dominated by products of largely effusive activity that have a trachyandesite basalt composition. This stage was also possibly responsible for the generation of occasional cinder cones with small flows, lava domes, and dykes of amphibole basaltic andesites.

The next stage gave rise to the generation of a 6 × 8 km caldera along the rim of the bounding scarp. The caldera bottom, with Lake Bol'shoe Gol'tsovoe inside, is also oval-shaped and is 4 × 6 km in size. Judging from the caldera size, its original depth might have been

Fig. 1. Geological–geomorphological map of the Kekuknai volcanic massif. (1) Accretion deposits of various origins: fluvioglacial, alluvial, lacustrine, etc. ($Q_3^4 - Q_4$); (2) moraines of the second phase of Late Pleistocene glaciation (Q_3^4); (3) eruptive centers (*a*, *c*) and flows (*b*, *d*) of trachybasalt–andesite, hawaiite–mugearite (*a, b*) and dacite–rhyolite (*c*, *d*) composition of the late stage of Holocene areal volcanism (Q_4); (4) eruptive centers (*a*) and flows (*b*) of trachybasalt (the early stage of areal volcanism) and hawaiite–mugearite (the middle stage of areal volcanism), of Middle–Late Pleistocene age ($Q_3^2 - Q_3^3$); (5) plateau basalts of Middle–Late Pleistocene age ($Q_2 - Q_3^1$); (6) trachyandesite–trachydacite extrusions of Early–Middle Pleistocene age (Q_{1-2}); (7) eruptive centers (*a*) and fragments of destroyed volcanic edifices (*b*) of trachybasalt–andesite basalt of the pre-caldera stage of Early–Middle Pleistocene age (Q_{1-2}); (8) volcanic rocks of Miocene–Pliocene basement (N_{1-2}); (9) explosive craters, maars, funnels of phreatic explosions on lava flows; (10) volcanic domes; (11) escarp of the volcanic–tectonic caldera; (12) faults, landfalls; (13) inferred faults.

Insert: position of the Kekuknai volcanic massif in the map of different-aged volcanic belts of the Kamchatka island-arc system. 1, $E_1 - E_2^2$ volcanic belt of western Kamchatka; 2, $E_3 - N_1$ and $N_2 - Q$ volcanic belts of Kamchatka (SR, Sredinnyi Range, SK south and EK eastern Kamchatka; 3, Kekuknai volcanic massif; 4, conventional boundaries of the central Kamchatka depression (CKD) and Aleutian–Kamchatka junction (AK).

1.5–2 km. Due to the caldera being infilled with later formations (thick lava sequences included), the depth of the caldera at present doesn't exceed 400–500 m. The products of the caldera-generating eruption itself have not been detected so far. During the closing phase of this stage, several extrusions of trachyandesites and trachydacites formed on the caldera's perimeter. They are well expressed in the topography as remnants 300 × 100 m to 800–900 × 300–400 m across at the base. The caldera supposedly formed in the Middle Pleistocene.

In the second half of the Pleistocene, a new phase of Kekuknai massif development commenced. In the SW parts of the area blanket basalts were formed[1] and products of superimposed areal volcanism formed a complex-structured lava shield (Dol Geologov) with many tens of individual eruption centers (lava and cinder cones and related flows). Some cones are from 0.1 to 1.5 km in diameter at the base, and from 20 to 150–200 m high. The flows associated with these reach 5–6 km in length. Based on volcanism mode and the distribution of volcanic products, this period is subdivided into three stages: early, middle, and late.

In the early stage of areal volcanism, olivine–clinopyroxene–plagioclase (with magnetite and spinel) trachybasalts of Middle–Late Pleistocene were formed. They compose cones with lava flows within the shield-like edifice on the caldera bottom and outside it in the NE part of the volcano. In addition, several eroded trachybasalts necks were found on the caldera rim.

The cones and related lava–pyroclastic flows of the middle stage of areal volcanism consist largely of olivine and olivine–clinopyroxene hawaiites, rarely of olivine–clinopyroxene (sometimes with plagioclase or orthopyroxene) mugearites and plagioclase–olivine–bipyroxene (with magnetite and spinel) basaltic andesites. Mugearites also compose two dykes in the southern part of Kekuknai Volcano. This stage correlates with the highest peak of areal volcanism, which formed the lava shield along the periphery of the volcano.

In the Late Pleistocene, destruction of the northern side of caldera occurred and a S–N trending riftogenic trough valley originated. In many respects this controlled the structural position of the youngest Holocene centers of the late stage of areal volcanism (see Fig. 1). Some cones are located inside the caldera or on its sides and also on the eastern and northern (Mount Chernaya) flanks of the trough valley; the associated flows partially infilled the caldera and the trough valley. The late stage of areal volcanism is represented in two rock associations: trachybasalt–andesite and hawaiite–mugearite, whose mineral composition is similar to that of the corresponding rocks generated during the first two stages of the areal volcanism. The peculiar volcanic center in the NE part of the area (see Fig. 1) also belongs to the late stage.[2] The center consists of four explosive craters 0.7 to 1.3 km across, which have discharged dacite and rhyolite pumice pyroclastic material. Then a rhyolite–dacite dome with a base area of about 0.8 km^2 and height about 100 m was formed there.

Dating the Volcanic Eruptions

In accordance with the data of geological mapping [*Ob"yasnitel'naya* ..., 1986, 1992], the shield edifice of Kekuknai Volcano is estimated to have formed in the Early Quaternary. Extrusive dacites and andesite–dacites are considered as Middle Quaternary rocks, while all forms of areal volcanism are classified as recent rocks of Holocene age. Age determinations by the 40Ar/39Ar method for basalts from the shield base of Bol'shoi Volcano, 1.7 ± 0.11 Ma and 1.86 ± 0.04 Ma, are given in [Volynets et al., 2010]. Carbon-14 dating of the youngest occurrence of rhyolite volcanism in

[1] The data on these basalts were obtained again in 2010 and are not considered in this paper.

[2] The data on these were also obtained again in 2010 and are not considered in this paper.

the NE part of the area gave an age of about 7200 years [Pevzner, 2004]. The results of our studies along with available age values and relationships with moraine deposits of the first phase of the Late Quaternary glaciation were used to develop a legend to the geological map of the Kekuknai massif (see Fig. 1)

Analytical Techniques

Rock-forming oxides were determined using an SRM-25 multichannel X-Ray spectrometer; Fe_2O_3 and FeO were separated by titration. Concentrations of trace elements were obtained by mass spectrometry with ionization in inductively coupled plasma (ICP-MS) at the Institute of Geochemistry of the Siberian Branch of the RAS. A detailed description of the sample preparation technique is given in [Yasnygina et al., 2003]. Measurements were carried out using a Plasma Quard 2+ (VG Elemental, UK) quadrupole mass spectrometer and a mass spectrometer with a magnetic sector ELEMENT 2 (Finnigan MAT, Germany). The values of the relative standard deviation varied from 0.3–0.8% (Sr, Zr, Cs, Nd, La) to 7–8% (Cr, Zn, Tm). The accuracy of the analysis was controlled according to international standards: BIR-1, BHVO-1, JB-2, BCR-2, DNC-1, RGM-1, and AGV-1. Comparison with the data [Volynets et al., 2010] obtained for samples with a similar composition from the same region demonstrated a good consistency between the results.

The isotope composition of the rocks was determined at the Vernadsky Institute of Geochemistry and Analytical Chemistry of the RAS, at the A.P. Vinogradov Institute of Geochemistry of the Siberian Branch of the RAS, and also in the Baikal Collective Use Analytical Center of the Siberian Branch of the RAS using standard techniques. Comparison with Sr isotope data obtained at Cornell University, USA and in the Geological Institute of the RAS [Volynets et al., 1995], as well as with materials on the isotopy of Sr, Nd, Pb [Volynets et al., 2010] in samples from the same area demonstrated good consistency between the results.

SOME FEATURES OF MATERIAL COMPOSITION

Petrogenic Elements. As seen from the data (Table 1, Fig. 2), the rocks of the Kekuknai volcanic massif exhibit a wide range of variations for most rock-forming oxides; however, extreme values of magmatic series compositions (high magnesium number, alkalinity, silica content) are not observed. Nonetheless, the rocks of each stage have compositions of their own.

In terms of alkalinity, all the rocks are potassium–sodium ($Na_2O/K_2O = 1.12–3.2$) with the exception of one high-sodium ($Na_2O/K_2O = 3.34$) basaltic andesite. At the same time, rocks of the pre-caldera and extrusive stages have low Na_2O/K_2O ratios of 1.12–1.8, while the rocks due to areal volcanism of all stages contain appreciably more sodium ($Na_2O/K_2O = 2.0–3.2$). This is the reason for application of a binary nomenclature marking hawaiites and mugearites among the occurrences of areal volcanism according to the formula $Na_2O - 2.0 \geq K_2O$ [*Klassifikatsiya* ..., 1997].

The $Na_2O + K_2O - SiO_2$ diagram (Fig. 2a) classifies the volcanic rocks of the pre-caldera and extrusive stages in a continuous trend from trachybasalts to trachydacites with some shift of cinder cone rocks into the field of basaltic andesites in the silica content range 54–56 wt %. Trachybasalts both from the early and the late stages of areal volcanism on this diagram occupy a position similar to those of the pre-caldera stage, but differ from the latter by higher concentrations of TiO_2 and extremely low values of SiO_2 and K_2O (Table 1, Fig. 2b). Significantly higher contents of total alkalinity are characteristic for the hawaiite–mugearite associations of the middle and late stages of areal volcanism (in the diagram of Fig. 2a these are located in the fields of trachybasalts and trachyandesite basalts, respectively). Norm nepheline occurs in these rocks, but its concentrations do not exceed 5–5.6%. A separate group is formed by a Pleistocene basaltic andesite association of the middle stage of areal volcanism, which has lower total and potassium alkalinity (see Figs. 2a and 2b) and contains norm quartz up to 4% and norm hypersthene (17–19%). Some samples even possess a real bipyroxene association. Here one also notes the above-mentioned rock compositions of the cinder cones of the pre-caldera stage and part of the compositions of basaltic andesite–andesite association of the late stage of areal volcanism. These rocks contain norm hypersthene (13–16%) and norm quartz (up to 6%).

In the $K_2O–SiO_2$ diagram (Fig. 2b), most figurative points of rocks of the pre-caldera and extrusive stages occur in the field of high-potassium rocks of the calc-alkaline type and form a common trend of direct correlative relation. That same field contains practically all the figurative points of the hawaiite–mugearite association of the middle stage and a considerable part of the compositions in the same association of the late stage of areal volcanism. For some rocks, the compositions from different associations occasionally pass into the shoshonite–latite field, but this feature has no genetic sense. On the other hand, two distinct anomalous minima of potassic alkalinity can be seen in the field of moderate potassium calc–alkaline rocks. One of these, in the range $SiO_2 = 53–58\%$, corresponds to the minimum of total alkalinity considered above (Fig. 2a), while the other occurred in trachybasalts of the earlier and late stages of areal volcanism. These anomalous fields, as well as the trend of the inverse correlative relation for rocks of different silica content of the middle stage of areal volcanism (Fig. 2b) do not fit the usual evolution scheme of volcanic series, but the causes of their origin can only be discussed after an analysis of all analytical material.

Trace element composition. As seen from Fig. 3, the distribution of trace elements in general, and rare-

earth elements in particular, for all evolutionary stages of the volcanic massif has an essentially similar character: a well-expressed Nb–Ta minimum and maxima of large-ion lithophiles and radioactive elements, as well as enrichment with light and depletion in heavy rare-earth elements (REE). One common feature in their distribution spectra consists in wide variations of the composition in the left parts of the diagrams and (at the level of Sm or Nd–Sm) an almost complete confluence of all curves with a well-expressed Y minimum. Nonetheless, each stage of the massif evolution involves some features of its own. Rocks of the pre-caldera and extrusive stages (see Figs. 3a and 3b) show minima of Nb, Ta, Zr, Hf, and Ti, and maxima of Rb, Ba, Pb, and St. These are usually thought to be related to fractionation of plagioclase-bearing parageneses at shallow depths and high saturation with fluids. A very weak europium minimum is observed in only one "anomalous in composition" extrusive trachyandesite (Sample 5-160). In rocks of the pre-caldera stage (Fig. 3a) there is one more "anomalous sample" (2621). It is peculiar in having higher concentrations of Nb and Ta and uncommonly low REE content starting from Sm. The rocks of the early stage of the Pleistocene areal volcanism distinctly divide into two groups (see Fig. 3c, Table 1). Less siliceous (SiO_2 = 46–47%), lower-magnesium, but higher calcium trachybasalts characteristically have lower concentrations of light REE (from La to Nd), Pb, Nb, Ta, Zr, and Hf, and are usually rich in Ba and Sr. More siliceous compositions (SiO_2 = 48.6–49.6%) on the contrary, differ by opposite characteristics for the same elements. Concentrations of Rb, Th, U, K, and Pb in trachybasalts of this stage are lower than in the same rocks of the pre-caldera stage, but in their concentrations of Nb and Ta, the rocks of both stages overlap significantly. Hawaiites and mugearites of the middle stage of areal volcanism are enriched in all elements of the left part of the diagram (see Fig. 3d–I) and light REE (see Fig. 3d–II) compared to trachybasalts of the early stage (Fig. 3c). The concentration of elements from Cs to K in most cases remains within the concentrations in rocks of the pre-caldera stage, while Nb, Ta, and light REE exceed these values. Basaltic andesites of the middle stage, in contrast to mugearites, have lower contents of alkalis, especially K. Thus, lower concentrations occur of such elements as Cs, Rb, Th, U, and light REE, as well as Nb and Ta. Volcanic rocks of the late stage of areal volcanism have a wide range of variations of element concentrations, both in the left part of the diagram (see Fig. 3e–I) and for REE (see Fig. 3e–II), thus generally mimicking the distribution of elements of the previous group (see Fig. 3d) with the exception of several analyses with low concentrations of Rb, Ba, Th, K, Nb, Ta, and Pb.

Judging by the distribution of trace elements (Fig. 3), the rocks of all associations that have been identified are close to island arc volcanic rocks, which becomes obvious by comparing them with the composition of the picrobasalts ("avachites") of Avacha Volcano [Koloskov, 2006], and they significantly differ from the same parameters for basanites in a subvolcanic body on Mount Khukhch [Perepelov et al., 2007b], which are of the "intraplate geochemical" type. However, an analysis of some indicator diagrams (Fig. 4) discloses substantial "non-island-arc" features in the composition of these volcanic rocks. The most representative in this respect are the Nb–K and Ta–K diagrams, which have good discriminating capabilities because the most fluid-mobile component (K) is compared with the least mobile (Nb and Ta), and the fields of basaltoids in different geodynamic settings are distinct. On the diagrams (Figs. 4a and 4b) the figurative points of the Kekuknai rocks form two sets. The trachybasalt–trachyandesite series of the pre-caldera stage and the trachyandesite–trachydacite series of the extrusive stage form a single series that is completely within the field of island arc volcanic rocks. The rocks of areal volcanism compose another series, with the trachybasalts of the Early Pleistocene stage occurring in the same island-arc field (from the previous group they differ only by notably lower potassium content), while the hawaiite–mugearite and andesite basalt rocks of the middle stage are completely outside its limits and are much closer to the field of Hawaiian volcanic rocks (the component of type-OIB basalts of oceanic islands), although they do not enter it. Basaltoids of the late Holocene stage have a scattered distribution, both inside the field of island arc rocks and outside it. It is important to emphasize that the MORB field (mid-oceanic ridge basalts) for the Pacific Ocean is separated from the values for the Kekuknai volcanic rocks, thus excluding the possible participation of this component in the petrogenesis of the rocks under discussion. The Nb–K diagram, in addition to our data, shows basalt compositions from the area of study taken from [Volynets et al., 2010].

The diagram demonstrates the good reproducibility of results obtained in different laboratories. The (La/Yb)n–K diagram is less informative (see Fig. 4c) because it compares components of almost the same mobility in the fluid flow; thus, a significant overlapping of all the fields; sometimes mistaken conclusions are made that, for example, a source of the "MORB type" is involved in island arc volcanic rocks. But even here, the same two series of rocks are defined occurring either in the island arc field or in the segment of overlapping fields.

In the K–Ti diagram (Fig. 4d) trachybasalts of the pre-caldera stage are located along the trend of geosynclinal (island arc) basalts. With the transition to trachyandesite basalts of this stage and extrusive trachyandesites and trachydacites, the figurative points shift toward decreasing titanium. The basalts of the areal type are rich in titanium and their figurative points shift toward the trend of the continental rifts, although they do not reach it. This probably is evidence of incipient rifting in the area.

Table 1. Content of petrogenic elements (wt %) and trace elements (g/t) in rocks of the Kekuknai massif

Stage	Pre-caldera													
Rock	tb	ga	tb	tb	tb	tb	tb	tab	ab	tab	tab	ab	ab	tab
Sample no.	5-161	2258	2737	2741	2604	G5-144	49072	5-141	2612	5-154-1	K-38-05	G-5-147	2621	K-44/1
##	1	2	3	4	5	6	7	8	9	10	11	12	13	14
SiO_2	48.55	48.88	49.18	49.91	50.35	50.37	50.65	52.38	52.47	53.98	55.12	55.37	55.93	56.04
TiO_2	1.08	1.79	1.04	1.05	1.10	0.93	1.04	0.94	1.02	0.86	0.96	0.99	0.86	0.73
Al_2O_3	18.14	18.59	17.10	17.70	19.25	18.27	18.88	18.39	18.50	17.59	18.26	18.51	16.32	18.28
F_2O_3	5.33	4.68	6.30	5.23	4.73	3.06	3.31	5.41	4.60	4.98	2.73	3.24	3.78	2.49
FeO	5.39	5.03	3.23	4.67	4.85	6.64	6.11	3.95	4.13	2.87	4.85	4.13	4.13	5.75
MnO	0.19	0.16	0.16	0.17	0.17	0.18	0.18	0.17	0.17	0.16	0.13	0.13	0.15	0.15
MgO	5.61	5.57	5.88	5.22	4.55	4.32	4.95	3.85	4.07	4.20	3.96	3.67	4.37	3.20
CaO	10.75	8.51	9.61	9.79	9.25	8.33	8.62	8.52	8.40	8.57	7.84	7.51	8.28	6.30
Ni_2O	2.81	4.11	2.58	2.87	3.07	3.33	3.16	3.01	3.35	3.36	3.66	3.56	3.02	3.99
K_2O	1.56	1.73	1.98	2.15	1.80	2.05	2.07	2.35	2.02	2.23	1.82	1.65	1.99	1.98
P_2O_5	0.35	0.55	0.43	0.50	0.41	0.41	0.43	0.51	0.38	0.43	0.32	0.30	0.24	0.34
LOI	0.27	0.55	2.18	1.68	0.48	2.42	0.51	0.62	0.52	0.19	0.40	1.12	0.45	0.86
Total	100.03	100.14	99.67	99.95	100.01	100.29	99.91	100.08	99.63	99.42	100.04	100.16	100.00	100.11
Cs	0.31	0.67	0.23	0.38	0.47	0.50	0.89	0.70	0.64	0.69	0.55	0.49	1.13	0.82
Rb	34	30	45	44	39	40	46	57	43	48	31	29	42	34
Ba	427	465	509	681	580	560	614	589	700	717	489	477	406	746
Th	1.10	2.22	1.01	1.25	1.58	1.50	1.79	1.76	2.23	1.73	2.23	2.37	3.71	2.01
U	0.59	1.03	0.85	0.95	0.98	1.04	1.13	1.57	1.14	1.15	0.87	0.86	1.42	1.16
Nb	2.4	23.6	3.1	3.5	4.9	3.72	5.3	3.3	5.6	4.3	8.16	8.66	11.0	4.13
Ta	0.15	1.40	0.22	0.25	0.32	0.24	0.34	0.25	0.40	0.28	0.53	0.58	0.80	0.27
La	8.12	24.85	10.25	11.80	13.50	11.50	14.23	13.90	14.94	11.07	15.65	17.08	14.45	12.59
Ce	21.99	54.46	26.09	29.03	33.13	27.92	34.98	34.74	36.00	27.87	33.82	36.75	30.61	29.21
Pb	3.4	3.1	4.6	4.4	7.8	5.29	6.7	5.0	5.3	6.3	3.67	4.38	5.0	6.44
Pr	3.31	7.06	3.70	4.22	4.63	3.84	4.93	4.95	4.87	4.22	4.18	4.58	3.89	3.84
Sr	646	792	672	630	788	709	733	713	631	642	637	647	435	700
P	1546	2393	1878	2188	1808	1773	1882	2205	1677	1873	1393	1328	1061	1485
Nd	15.91	28.03	16.89	18.64	20.86	17.48	22.07	21.62	21.52	19.40	17.77	18.15	15.53	16.12
Zr	80	230	102	96	122	96	145	131	130	103	63	59	92	100
Hf	1.96	4.90	2.68	2.63	2.99	2.44	3.43	3.36	3.29	2.66	3.24	3.54	2.35	2.57
Sm	4.21	5.91	4.21	4.51	5.21	4.38	5.33	5.39	4.94	4.45	3.97	4.04	3.40	3.69
Eu	1.35	1.87	1.38	1.42	1.65	1.39	1.67	1.65	1.57	1.39	1.22	1.23	1.06	1.15
Gd	4.02	5.34	3.97	3.89	4.92	4.19	4.81	4.99	4.44	4.20	3.56	3.77	3.09	3.38
Ti	6449	10743	6198	6281	6605	5539	6240	5605	6132	5138	5743	5898	5126	4383
Tb	0.62	0.80	0.62	0.61	0.77	0.65	0.74	0.77	0.70	0.68	0.55	0.58	0.49	0.51
Dy	3.74	4.69	3.71	3.69	4.59	3.93	4.32	4.48	4.20	4.52	3.33	3.41	2.95	3.03
Y	20	26	19	21	23	21	23	22	24	20	17	18	17	16
Ho	0.75	0.92	0.74	0.77	0.90	0.78	0.86	0.87	0.86	0.89	0.68	0.68	0.61	0.61
Er	2.03	2.42	2.00	2.13	2.44	2.16	2.38	2.41	2.34	2.85	1.86	1.90	1.72	1.68
Tm	0.30	0.34	0.30	0.31	0.37	0.32	0.35	0.37	0.35	0.36	0.27	0.27	0.26	0.24
Yb	1.88	2.19	1.89	2.02	2.35	2.01	2.23	2.28	2.27	2.44	1.70	1.74	1.58	1.60
Lu	0.28	0.33	0.28	0.29	0.35	0.31	0.34	0.35	0.34	0.36	0.26	0.26	0.24	0.25

Table 1. (Contd.)

Stage	Extrusive						Early stage of areal volcanism							
Rock	tab	ta	ta	ta	ta	ta	tb	tb	tb	tb	tb	tb	ga	tb
Sample no.	K-40-05	5-160-1	K-39	44-05	5-160	5-152	53-05	53-05a	52-05	2745	2747	49057	57-05	49058
##	15	16	17	18	19	20	21	22	23	24	25	26	27	28
SiO_2	55.48	57.90	60.15	60.47	60.84	61.95	46.26	46.26	46.42	46.52	47.16	48.59	49.40	49.56
TiO_2	0.98	0.73	0.47	0.61	0.76	0.42	1.24	1.24	1.26	1.43	1.73	1.44	1.37	1.40
Al_2O_3	18.43	18.31	18.46	17.97	17.89	17.89	17.70	17.70	17.90	18.21	17.63	17.24	16.95	17.72
Fe_2O_3	3.29	4.05	2.42	5.57	4.26	4.75	6.28	6.28	4.75	3.65	4.83	5.63	4.86	5.16
FeO	3.95	2.69	3.41	0.36	1.08	0.22	5.03	5.03	6.59	7.18	6.11	4.49	5.21	4.85
MnO	0.12	0.16	0.20	0.14	0.15	0.18	0.18	0.18	0.19	0.17	0.16	0.16	0.16	0.16
MgO	3.59	2.54	1.72	1.71	1.64	1.43	6.86	6.86	6.73	6.86	6.98	7.35	7.41	7.02
CaO	7.34	5.96	5.04	4.64	4.14	4.73	12.06	12.06	12.17	11.46	10.79	9.82	9.49	9.39
N_2O	3.67	4.06	4.17	4.31	4.47	4.10	2.66	2.66	2.64	2.50	2.99	3.22	3.36	3.12
K_2O	1.73	2.66	2.71	2.54	4.09	2.81	1.06	1.06	0.91	0.94	0.90	1.11	1.10	1.17
P_2O_5	0.29	0.39	0.29	0.33	0.44	0.26	0.35	0.35	0.31	0.27	0.27	0.31	0.35	0.35
LOI	0.93	0.53	0.94	1.38	0.27	1.14	0.39	0.39	0.14	0.55	0.35	0.48	0.51	0.07
Total	99.81	99.97	99.97	100.03	100.02	99.87	100.07	100.07	100.00	99.73	99.89	99.85	100.17	99.96
Cs	0.53	1.06	0.72	0.82	1.70	0.99	0.44	0.25	0.56	0.35	0.23	0.26	0.25	0.14
Rb	30	59	49	61	98	57	27	17	30	18	12	15	18	17
Ba	494	784	760	866	1159	885	436	441	479	146	208	231	265	274
Th	2.55	2.16	1.70	2.06	3.84	2.41	0.81	0.83	0.79	0.52	0.70	0.99	1.07	1.02
U	0.94	1.59	1.13	1.29	2.84	1.55	0.41	0.45	0.41	0.32	0.26	0.42	0.42	0.42
Nb	9.16	4.9	5.14	4.7	10.2	5.4	4.6	3.6	4.4	6.2	9.2	9.4	8.7	10.3
Ta	0.59	0.33	0.33	0.33	0.67	0.39	0.36	0.20	0.31	0.37	0.52	0.48	0.51	0.61
La	17.04	15.24	15.27	15.89	23.26	16.30	9.56	8.61	8.76	9.79	9.88	15.35	14.38	15.15
Ce	35.67	34.80	35.67	36.20	53.49	36.75	25.28	22.26	22.97	24.71	25.10	32.51	32.35	34.20
Pb	4.86	7.4	7.64	6.4	10.8	8.0	2.0	1.8	2.1	1.1	1.4	2.4	2.3	2.3
Pr	4.60	4.73	4.69	4.78	7.89	4.83	3.72	3.23	3.41	3.45	3.68	4.19	4.29	4.52
Sr	668	667	692	612	500	678	634	580	646	566	512	512	535	540
P	1275	1690	1258	1450	1913	1131	1546	1546	1341	1157	1188	1371	1528	1507
Nd	18.78	20.66	19.66	20.26	33.01	20.57	16.98	14.55	16.37	15.78	16.70	17.17	18.19	19.04
Zr	152	150		152	225	157	83	71	74	97	103	129	115	133
Hf	3.54	3.17		3.28	5.15	3.38	2.14	1.93	2.15	2.48	2.70	3.03	2.74	3.28
Sm	4.11	4.42	4.15	4.45	6.82	4.39	4.65	4.19	4.35	4.01	4.01	4.23	4.18	4.45
Eu	1.25	1.38	1.30	1.37	1.68	1.37	1.51	1.42	1.45	1.31	1.35	1.38	1.33	1.44
Gd	3.71	4.03	3.71	4.10	6.64	3.96	4.24	4.08	4.39	4.04	4.09	4.17	3.94	4.16
Ti	5892	4341	2796	3659	4533	2521	7419	7419	7563	8569	10353	8641	8228	8377
Tb	0.57	0.60	0.56	0.64	0.87	0.60	0.63	0.62	0.65	0.61	0.66	0.63	0.59	0.65
Dy	3.47	3.57	3.35	3.74	6.15	3.41	3.62	3.59	3.73	3.78	3.97	3.76	3.51	3.94
Y	17.96	23	17.94	22	29	19	19	18	18	20	21	21	19	21
Ho	0.71	0.73	0.66	0.75	1.23	0.70	0.69	0.66	0.71	0.77	0.81	0.77	0.72	0.80
Er	1.90	1.96	1.80	2.05	3.55	1.88	1.85	1.80	1.87	2.13	2.19	2.09	1.97	2.16
Tm	0.28	0.28	0.27	0.31	0.51	0.28	0.27	0.26	0.28	0.32	0.32	0.30	0.29	0.32
Yb	1.78	1.84	1.68	1.94	3.42	1.76	1.72	1.71	1.79	1.98	1.99	1.90	1.90	2.02
Lu	0.27	0.28	0.26	0.30	0.52	0.27	0.26	0.26	0.27	0.30	0.29	0.27	0.29	0.30

Table 1. (Contd.)

Stage	Early stage of areal volcanism													
Rock	ga	ga	ga	tb	ga	ga	ga	ga	ga	ga	ga	ga	ga	mug
Sample no.	5-155	49067	2614	2616	49071	49065	G-5-162	PP-2751	PP-2752	III-2753	IP-274	5-152-1	49070	G-5-153
##	29	30	31	32	33	34	35	36	37	38	39	40	41	42
SO_2	48.51	48.69	49.26	49.26	49.38	49.41	49.56	50.24	50.50	50.73	50.86	51.02	51.05	52.99
TiO_2	1.89	1.94	1.98	1.98	1.90	1.68	1.69	1.89	1.88	1.90	1.64	1.69	1.57	1.41
Al_2O_3	17.54	18.73	17.88	18.46	19.14	18.60	17.65	18.79	18.88	18.74	17.76	17.94	18.63	17.30
Fe_2O_3	4.63	5.86	4.25	4.39	3.80	2.63	4.35	6.19	5.02	4.89	5.11	4.66	4.76	4.25
FeO	5.21	4.67	5.57	5.39	6.47	7.18	5.56	4.13	5.21	5.21	4.67	4.31	5.03	3.95
MnO	0.15	0.15	0.15	0.15	0.16	0.16	0.15	0.16	0.16	0.16	0.16	0.15	0.17	0.14
MgO	6.22	4.87	5.82	5.34	4.48	5.20	6.39	3,94	3.85	3.98	5.19	4.59	3.86	5.14
CaO	9.60	8.15	8.03	8.03	7.57	8.83	8.22	6.94	6.97	7.01	7.92	8.24	7.16	7.76
Na_20	4.08	4.36	4.09	4.17	4.61	4.10	4.10	4.92	4.88	4.74	3.99	4.35	4.81	4.26
K_20	1.37	1.73	1.96	2.08	1.73	1.43	1.67	1.78	1.81	1.82	1.60	1.98	1.91	2.00
P_2O_5	0.54	0.54	0.49	0.48	0.41	0.35	0.51	0.43	0.42	0.43	0.36	0.58	0.53	0.41
LOI	0.28	0.18	0.16	0.28	0.43	0.25	0.22	0.51	0.47	0.16	0.37	0.42	0.40	0.49
Total	100.00	99.86	100.12	100.01	100.08	99.83	100.07	100.19	100.11	99.75	99.61	99.92	99.87	100.10
Cs	0.67	0.28	0.31	0.43	0.83	0.50	0.29	0.51	0.52	0.70	0.34	1.00	0.61	0.68
Rb	33	24	27	23	30	20	20	31	29	33	23	42	29	39
Ba	501	607	522	484	331	324	345	444	422	362	338	645	379	584
Th	2.41	1.05	1.13	0.84	1.45	1.48	1.69	2.17	1.91	1.92	1.67	3.39	1.61	4.66
U	0.90	0.37	0.48	0.34	0.60	0.49	0.68	0.81	0.70	0.74	0.69	1.44	0.72	1.65
Nb	18.9	17.7	17.2	13.9	18.4	14.8	23.3	26.3	23.6	22.7	14.8	26.5	18.0	23.6
Ta	1.09	1.04	0.97	0.84	1.01	0.88	1.31	1.39	1.31	1.24	0.80	1.37	0.94	1.44
La	25.15	20.02	23.08	16.54	19.99	16.41	19.45	20.10	19.00	19.60	17.21	30.69	19.10	27.29
Ce	56.66	48.56	54.16	39.75	44.70	37.62	43.51	46.00	43.60	43.89	40.10	64.56	45.18	56.94
Pb	3.3	2.6	2.4	2.4	2.4	2.6	2.6	2.1	2.1	3.6	2.9	6.5	2.9	6.1
Pr	7.10	6.85	7.03	5.44	5.63	4.76	5.62	6.07	5.53	5.51	5.20	7.92	5.90	7.17
Sr	799	830	699	756	810	653	701	757	735	855	657	844	718	616
P	2336	2341	2127	2100	1808	1546	2223	1869	1812	1860	1550	2546	2297	1803
Nd	29.30	29.57	28.94	23.18	23.04	19.67	23.14	24.99	23.47	22.25	21.96	31.44	25.40	28.09
Zr	208	191	182	162	153	121	182	177	163	174	133	263	187	231
Hf	4.57	4.47	4.42	4.04	3.46	2.98	4.01	4.04	3.64	3.76	2.69	5.36	3.79	4.84
Sm	6.17	6.51	6.07	5.56	4.76	4.35	5.20	5.25	4.97	5.04	4.77	6.49	5.64	5.53
Eu	1.88	2.00	1.87	1.72	1.52	1.39	1.64	1.69	1.53	1.58	1.52	1.88	1.77	1.68
Gd	5.37	5.54	5.22	4.97	4.48	4.14	4.72	4.70	4.34	4.45	4.40	5.18	5.21	5.45
Ti	11287	11605	11826	11850	11353	10042	10126	11293	11251	11353	9802	10096	9377	8449
Tb	0.79	0.84	0.78	0.74	0.67	0.66	0.71	0.70	0.65	0.70	0.67	0.79	0.81	0.82
Dy	4.50	5.04	4.61	4.29	4.03	3.92	4.08	4.45	4.04	4.18	4.00	4.78	4.64	5.06
Y	25	28	25	20	22	20	20	25	22	23	20	26	23	22
Ho	0.86	0.99	0.91	0.81	0.79	0.78	0.79	0.89	0.80	0.85	0.78	0.97	0.89	1.01
Er	2.25	2.65	2.43	2.09	2.12	2.06	2.04	2.47	2.23	2.25	2.06	2.69	2.40	2.70
Tm	0.32	0.39	0.34	0.30	0.30	0.30	0.30	0.37	0.33	0.32	0.29	0.39	0.35	0.39
Yb	1.98	2.48	2.15	1.81	1.95	1.90	1.89	2.37	2.12	2.01	1.84	2.50	2.16	2.57
Lu	0.30	0.36	0.33	0.27	0.31	0.29	0.29	0.34	0.32	0.30	0.28	0.38	0.33	0.38

Table 1. (Contd.)

Stage	Middle stage of areal volcanism				Late stage of areal volcanism										
Rock	mug	ab	ab	ab	tb	tb	tb	ga	ga	ga	tb	mug	mug	mug	ab
Sample no.	G-5-154	k-41-05	49064	G-5-138	K-48-05	49061	49060	K-43-05	pp 2627	G-5-158	49055	G5-163	49051	IP-2602	IP-2608
##	43	44	45	46	47	48	49	50	51	52	53	54	55	56	57
SiO_2	54.29	54.52	55.00	55.26	47.09	47.27	48.71	49.51	49.75	51.86	51.92	52.27	52.93	55.41	56.73
TiO_2	1.32	1.21	1.14	1.24	1.15	1.48	1.48	1.47	1.49	1.56	1.24	1.18	1.17	1.08	1.36
Al_2O_3	17.42	17.43	17.22	17.13	16.20	18.64	18.65	17.48	17.83	18.34	17.77	17.43	16.93	17.61	18.00
Fe_2O_3	4.98	2.85	2.57	3.05	5.13	2.76	4.57	4.46	4.80	5.23	2.55	3.86	4.76	2.81	3.30
FeO	2.87	5.21	5.21	4.85	5.39	7.72	5.75	5.39	5.21	4.67	6.29	5.21	3.95	4.85	4.31
MnO	0.15	0.13	0.13	0.13	0.17	0.17	0.16	0.16	0.17	0.17	0.16	0.15	0.16	0.15	0.11
MgO	4.35	4.62	4.72	4.82	9.05	6.31	5.59	6.86	6.62	4.02	5.45	5.51	5.46	3.95	2.97
CaO	7.27	7.45	7.45	7.48	11.58	10.93	9.80	8.60	8.43	7.07	8.72	8.03	8.21	6.57	6.43
Na2O	4.49	3.79	3.90	3.61	2.49	2.98	3.37	3.71	3.62	4.54	3.57	3.99	3.94	4.59	4.28
K_2O	2.13	1.59	1.50	1.48	1.02	1.14	1.38	1.44	1.47	1.74	1.78	1.86	1.82	2.18	1.28
P_2O_5	0.39	0.43	0.41	0.41	0.32	0.29	0.36	0.47	0.52	0.52	0.27	0.26	0.27	0.32	0.31
LOI	0.44	0.44	0.66	0.44	0.41	0.37	0.22	0.24	0.27	0.41	0.37	0.41	0.43	0.18	0.49
Total	100.10	99.66	100.03	99.90	100.00	100.05	100.05	99.79	100.16	100.12	100.10	100.16	100.02	99.70	99.57
Cs	0.75	0.36	0.38	0.29	0.43	0.44	0.33	0.51	0.47	0.76	0.38	0.86	0.97	0.84	0.30
Rb	43	20	27	21	23	24	28	24	26	27	32	30	38	39	18
Ba	618	443	476	583	472	181	293	348	388	375	319	338	416	501	343
Th	4.77	2.06	2.66	2.21	1.99	0.68	1.07	1.09	1.31	1.45	2.02	2.86	2.82	3.22	1.87
U	1.87	0.68	0.88	0.78	0.45	0.39	0.53	0.45	0.59	0.64	0.81	0.97	0.96	1.17	0.57
Nb	23.9	13.0	14.7	12.2	5.5	7.7	11.3	13.9	15.3	16.8	12.5	13.79	16.9	19.6	12.9
Ta	1.49	0.74	0.77	0.74	0.33	0.43	0.59	0.82	0.76	0.95	0.71	0.84	1.06	1.17	0.83
La	28.89	18.37	21.86	21.67	10.20	11.37	13.69	17.27	20.91	18.51	17.92	18.60	24.39	26.19	20.84
Ce	58.99	43.73	47.91	48.87	26.31	27.97	33.01	41.61	44.26	41.77	37.62	39.61	50.32	55.38	42.81
Pb	6.8	4.4	4.5	5.7	2.3	1.4	2.5	2.6	3.1	2.6	2.5	3.20	2.8	3.6	3.5
Pr	7.19	5.68.	6.12	6.73	3.83	3.97	4.55	5.42	5.83	5.59	4.78	5.09	5.92	6.63	5.17
Sr	603	607	536	595	556	618	586	611	620	705	453	396	414	428	570
P	1707	1869	1777	1795	1406	1279	1563	2039	2249	2262	1166	1153	1179	1415	1371
Nd	29.06	24.47	23.53	27.55	17.48	17.80	20.13	23.02	22.61	23.84	19.00	20.46	23.16	25.66	21.28
Zr	244	165	190	179	86	114	134	158	169	178	158	67	190	212	171
Hf	4.72	3.58	4.34	3.94	2.63	2.46	3.42	3.49	3.33	3.52	3.51	3.40	3.70	4.76	4.59
Sm	5.64	5.02	4.88	5.67	4.34	4.60	4.59	5.06	5.35	5.53	4.37	4.31	4.56	4.89	4.48
Eu	1.70	1.59	1.49	1.70	1.45	1.50	1.50	1.62	1.67	1.70	1.42	1.39	1.38	1.53	1.43
Gd	5.42	4.79	4.39	5.57	4.56	4.42	4.57	4.52	4.96	4.91	4.04	4.06	3.99	4.40	4.08
Ti	7898	7257	6844	7437	6868	8868	8880	8820	8892	9329	7443	7078	7024	6443	8138
Tb	0.80	0.72	0.64	0.72	0.69	0.69	0.70	0.71	0.77	0.75	0.64	0.62	0.59	0.66	0.60
Dy	5.03	4.36	3.81	5.03	4.08	4.12	4.29	4.18	4.34	4.47	3.80	3.85	3.58	3.81	3.51
Y	22	18	20	21	19	21	21	21	25	23	20	21	23	20	19
Ho	0.98	0.80	0.76	0.90	0.89	0.82	0.83	0.84	0.87	0.86	0.75	0.76	0.75	0.76	0.68
Er	2.69	2.18	2.11	2.54	2.54	2.17	2.17	2.29	2.26	2.26	2.05	2.07	2.11	2.16	1.84
Tm	0.37	0.30	0.31	0.37	0.34	0.31	0.32	0.35	0.33	0.32	0.30	0.30	0.31	0.33	0.27
Yb	2.52	1.94	1.93	2.38	2.20	1.94	2.06	2.25	2.09	2.00	1.95	1.88	2.00	2.11	1.65
Lu	0.38	0.27	0.29	0.36	0.31	0.29	0.31	0.33	0.30	0.30	0.30	0.29	0.30	0.31	0.24

a

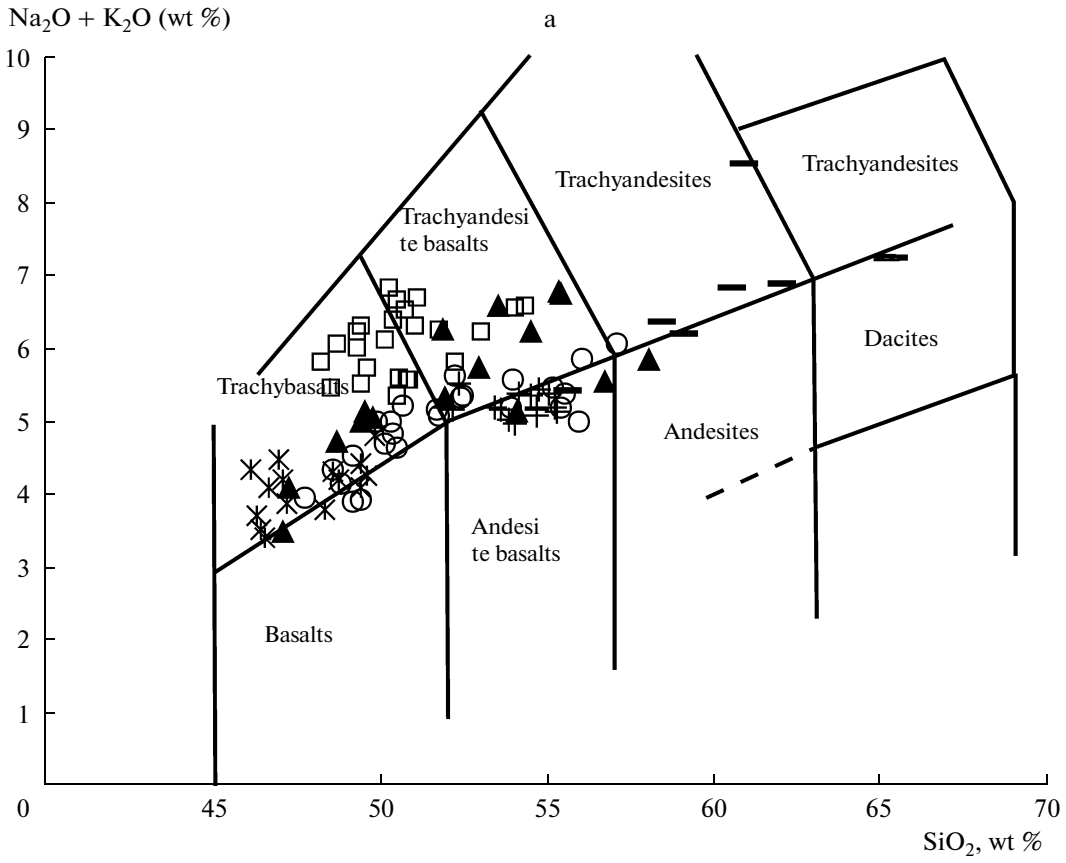
Na2O + K2O (wt %)
10
9
8
7
6
5
4
3
2
1
0
45
50
55
60
65
70
SiO2, wt %
Trachyandesites
Trachyandesites
Trachyandesi
te basalts
Dacites
Trachybasalts
Andesites
Andesi
te basalts
Basalts

b

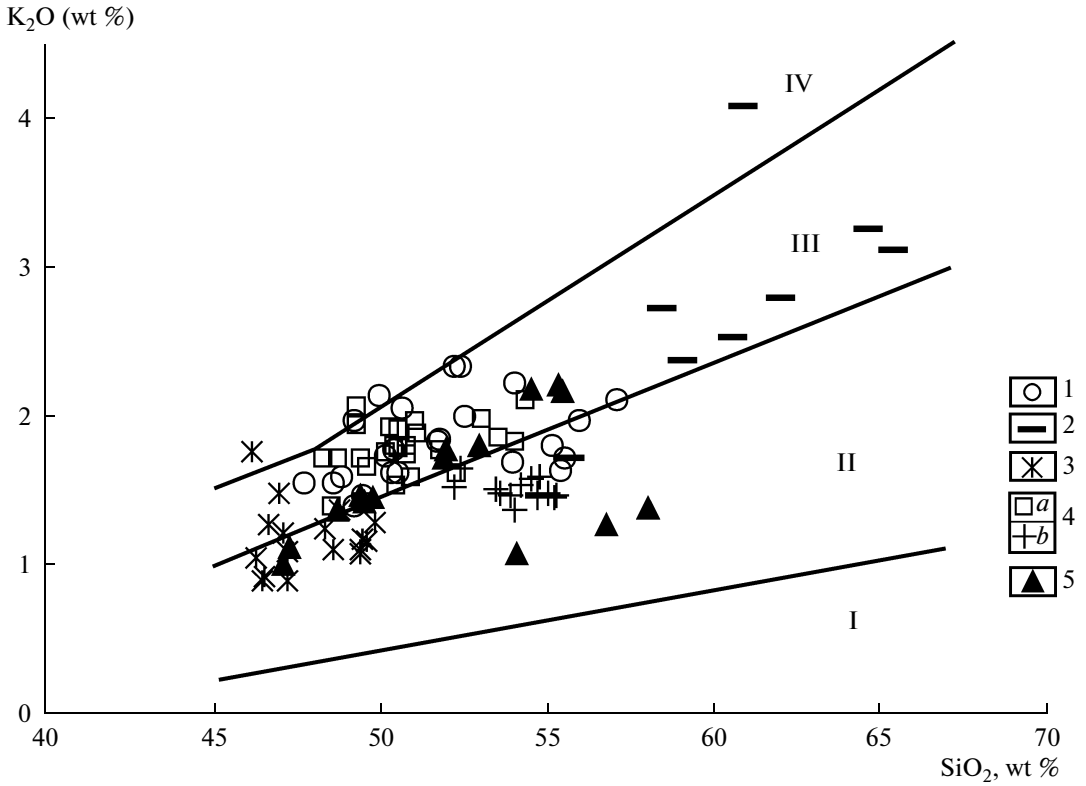
K2O (wt %)
4
3
2
1
0
40
45
50
55
60
65
70
SiO2, wt %
IV
III
II
I
1
2
3
4
a
b
5

It should be noted that all diagrams show coincidence (complete or partial) of figurative points of composition of the areal volcanism with the fields of intraplate geochemical rocks identified in the plateau basalts of the Ichinskii and Bakening Volcanoes [Koloskov, 2006] as well as with the fields of the "Columbia River" basalts, which are a typical example of continental plateau basalts in a backarc volcanic basin [Hooper and Hawkesworth, 1993; Smith, 1992].

Isotope characteristics. The isotope composition of the Kekuknai rocks varies insignificantly (Table 2) and involves overlapping for most of its evolution stages; the composition differs considerably from similar parameters of Miocene basanites of "intraplate geochemical" type. In addition, the previously determined [Volynets et al., 1995] isotope composition of Sr in basalts of Dol Geologov (the zone of areal volcanism of the Kekuknai massif) varies within $^{87}Sr/^{86}Sr = 0.703113–0.70337$, which is practically within the values presented in Table 2. These are very important remarks attesting to the fact that the Kekuknai rocks have been little affected by secondary alterations and their evolution was connected with that of a single isotopic system.

DISCUSSION OF MATERIALS

One of the most important points from which to start this discussion is probably the problem of combined island-arc and intraplate geochemical types with possible convergence of the respective features in a non-typical geodynamic setting. Volynets et al., [1986] classify subalkaline basalts–basaltic andesites of Kekuknai Volcano as belonging to a high potassium calc-alkaline series (HPCAS) with island-arc peculiarities in the REE distribution. Those authors classified only potassium alkaline rocks of western Kamchatka as intraplate. Subsequent publications [Volynets et al., 1995; Volynets, 1994] treated the Dol Geologov basalts as an intraplate geochemical type whose generation was modeled so as to involve mantle plumes. The origin of volcanic rocks with island-arc features was considered within the framework of the subduction model. Finally, one of the more recent works [Volynets et al., 2010] treats the Kekuknai "monogenic field" (due to areal volcanism) rocks as belonging to a high potassium basalt series with intraplate features. Their origin was explained on the basis of the subduction model involving three components: a MORB source, an enriched mantle source, and fluids from the underthrusting oceanic plate.

Analysis of the diagrams in Fig. 4 attests to the presence of island arc and intraplate geochemical types in the rocks of the Kekuknai massif. The island arc volcanic rocks are so much separated from the MORB field by their major integration features (see Figs. 4a and 4b) that the associated source could not have participated in their petrogenesis, while the intraplate volcanic rocks, on the contrary, are close to the OIB field but differ in having higher potassium alkalinity. This circumstance may attest to participation of a metasomatically enriched Hawaiian-type mantle reservoir in the generation of the respective source melts.

Let us consider the transition between these geochemical rock types during the evolution of the Kekuknai volcanic structure.

As shown on the multicomponent diagram and in the plot of REE concentrations (see Fig. 3), the main differences among the volcanic rocks produced during different stages of the Kekuknai massif evolution are largely determined by the composition and concentration of fluid-mobile elements (including light REE). These peculiarities are especially clear in the plots of correlation of fluid-mobile elements relative to the non-mobile component in the fluid stage (Fig. 5). The indications of the $Yb_n–Ce_n$ diagram were considered in our analysis of compositions of Late Cretaceous–Paleocene magmatic complexes in central Kamchatka [Koloskov et al., 2009]. The correlative accumulation of both components on the diagram is governed by processes of fractional crystallization in accordance with the fractionation trend for the well-known Skaergaard massif [McBirney, 2002]. Figurative points of the Kekuknai rocks form a field that is elongate toward the fluid-mobile Ce, thus falling in the field of metasomatically altered deep spinel peridotite xenoliths [Koloskov et al., 2009]; when Yb increases slowly, it accumulates largely in fractionation processes (or changed selective melting). Therefore, we suppose that the leading mechanism that was responsible for changes in composition for different stages of Kekuknai massif evolution was the dynamics of the fluid phase supplemented by fractional crystallization inside individual stages.

Based on the ytterbium content in rocks as an indicator of the degree of fractionation (the advance in the evolutionary series), we compiled generalized diagrams to depict the behavior of the relatively immobile elements Ti and Nb in the fluid phase (Fig. 6) and components that are easily transported by fluids (Pb,

Fig. 2. Ratio $(Na_2O + K_2) – SiO_2$ (a) and $K_2O – SiO_2$ (b) in rocks of the Kekuknai massif. (1) Trachybasalt–andesite basalt association of the pre-caldera stage; (2) extrusive trachyandesite–trachydacite association; (3) trachybasalt association of the early stage of the Pleistocene areal volcanism; (4) hawaiite–mugearite (*a*) and andesite basalt (*b*) association of the middle stage of the Pleistocene areal volcanism; (5) trachybasalt–andesite and hawaiite–mugearite associations of the late stage of the Holocene areal volcanism. Classification diagrams after [*Petrograficheskii ...*, 2009] (a) and [Peccerillo and Taylor, 1976], with addition from [*Petrologiya ...*, 1987] (b). Roman numerals denote fields of the following series: low-potassium (I), moderately potassium calc-alkali (II), high potassium calc-alkali (III), and subalkaline (IV).

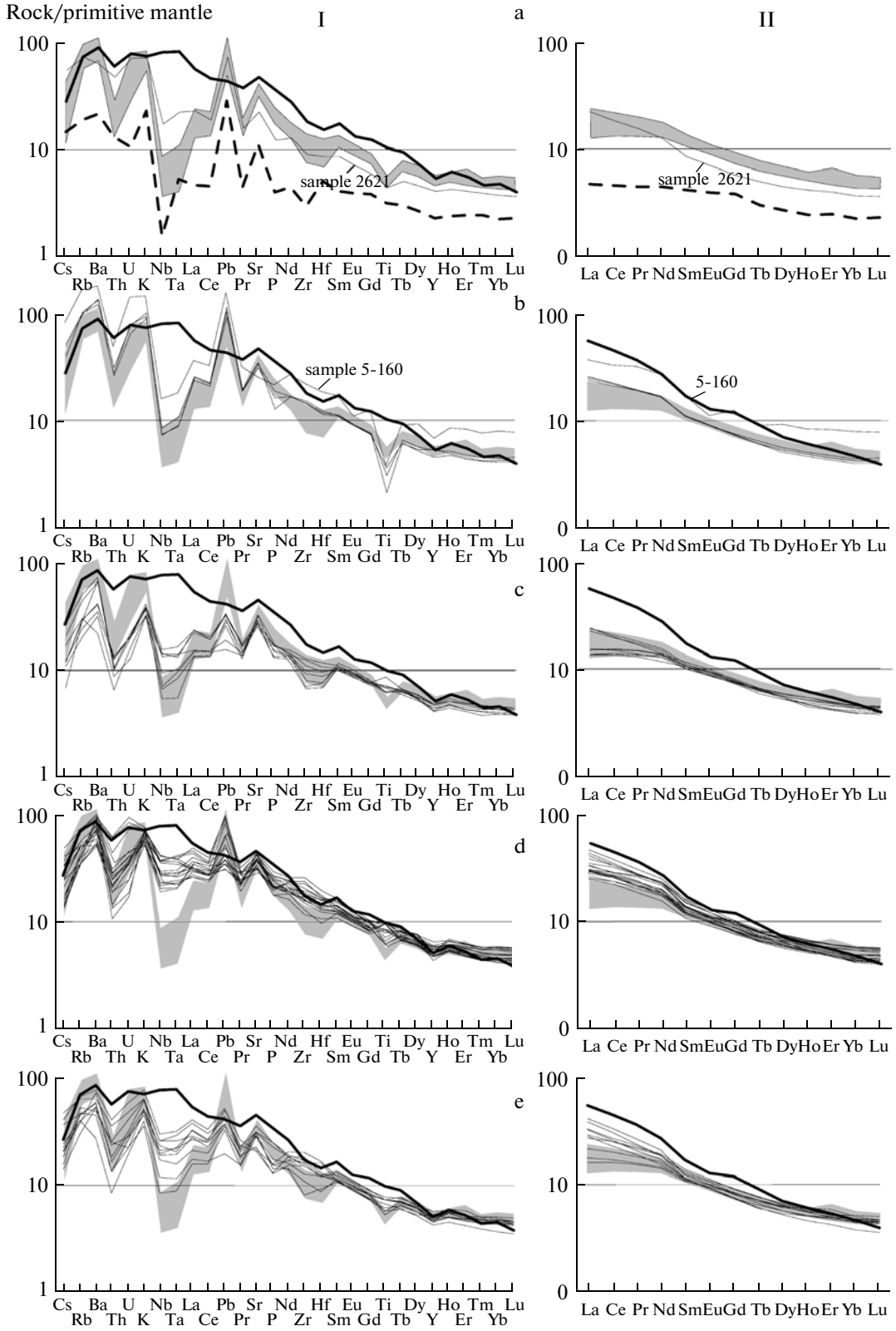

Rb, Ba, Th, K, and Sr) (Fig. 7) in the course of evolution of the fluid–magmatic system under consideration. The pre-caldera and extrusive stages of this system's evolution were accompanied by successive accumulation of all fluid-mobile components (K, Rb, Ba, Pb, and Th), as well as light REE, and some high-charge elements (Nb, Zr, and Hf) on the background of increasing silica content (see Figs. 6-I, 6-II, 7-I,

Fig. 3. Multicomponent diagram of the distributions of elements (I) and graph of normalized concentrations of REE (II) in rocks of the Kekuknai massif. (a) Trachybasalt–andesite basalt association of the pre-caldera stage; (b) extrusive trachyandesite–trachydacite association; (c) trachybasalt association of the early stage of the Pleistocene areal volcanism; (d) hawaiite–mugearite and andesite basalt association of the middle stage of the Pleistocene areal volcanism; (e) trachybasalt–andesite and hawaiite–mugearite associations of the last stage of areal (Holocene) volcanism. On all the diagrams the dark background highlights the field of compositions of the pre-caldera stage, the heavy solid line denotes the average basanite composition of Mount Khukhch [Perepelov et al., 2007b], the dashed line denotes the picrobasalts of Avacha Volcano [Koloskov, 2006]. For explanations, see main text. The concentrations of elements in rocks are normalized by their content in pyrolite (primitive mantle) after [Sun and McDonough, 1989].

and 7-II; Table 1) and probably of total water saturation of the melts resulting from both the additional infusion of fluids and fractional differentiation. The Ti content was decreasing during this process (see Figs. 6a-I and 6a-II), which is explained by the early fractionation of titanomagnetites; at the same time Sr (see Figs. 7f-I and 7f-II) behaves in a stable manner because the element is less fluid mobile, while fractionation of clinopyroxene and plagioclase was compensated by the increasing involvement of feldspars in the rock matrix.

At some moment the volatile elements accumulated to a certain critical amount and the system "exploded." Together with the separation of volatiles, many fluid-mobile components are removed (fluid extraction), which is reflected in the composition of rocks during the early stage of areal volcanism (see Fig. 7-III, Table 1). Here, sharply lower concentrations of all fluid-mobile elements (K, Rb, Ba, Pb, Th, and light REE) are observed; the content of "passive" Sr remains stable, while the concentrations of high-charge elements (Nb, Ta, Ti, and Hf) either remain at the same level or increase, possibly due to transition from oxidizing to reducing conditions in the system (instead of titanomagnetites, the first to crystallize are chrome–aluminous spinels). The potassium minimum is especially expressed (see Fig. 7e-III); the minimum was already noted when analyzing the K_2O–SiO_2 diagram (see Fig. 2b) in the range SiO_2 = 46–50 wt %. The behavior of Zr is of interest (see Table 1); its concentration is also decreased probably due to its "affinity" with silica, because the change in composition occurs there on the background of a sharp drop in the silica content in the rocks.

The middle stage of areal volcanism corresponds to a new stage in the evolution of the fluid–magmatic system controlled by further accumulation of volatile components and the advanced fractionation. In the hawaiite–mugearite rock association, we note successively increasing concentrations of fluid-mobile elements (see Fig. 7-IVa) and increasing content of Nb (see Fig. 6-IVa) as well as of Ta and Zr (see Table 1). The content of the latter, as before, is determined by increasing silica concentration in the rocks, but drops in bipyroxene basaltic andesites, probably due to contamination by crustal material. The Ti content is in general high (see Fig. 6-IVa) but decreases during fractionation of the melts and transition to the basaltic andesite association (see Fig. 6-IVb). At this stage the volcanic rocks acquire an appearance of the "intraplate geochemical type." This is probably due to the great depth of melting and a largely reducing composition of the fluids being introduced, because in these rocks the first to crystallize are not titanomagnetites but chrome–aluminous spinels in association with olivine, whose fractionation little affects the concentrations of high-charge elements. At the middle stage the basaltic andesite association shows another minimum concentration of fluid-mobile components (see Fig. 7-IVb and the second potassium minimum in the diagram of Fig. 2b), and high-charge elements (see Fig. 6-IVb). As long as this minimum is noted in rocks of high silica content and is accompanied by an "anomalous" bipyroxene association of phenocrysts, it may be explained by significant contamination of the rocks by crustal material. It is worth noting that the respective field in the generalized diagrams showing the change in element concentrations (see Figs. 6-IVb and 7-IVb) may be extrapolated to cover the basaltic andesites of Mount Chernaya (see Figs. 6-V and 7-V, analysis 57; Table 1, sample 2608), which are saturated with gabbro–gabbrodiorite xenoliths. Low Zr concentration is also noted there, not in conformity with the increasing silica content (see Table 1, sample 56). It should be emphasized that the geochemical controls of dykes and necks are significantly different: in dykes the process of crystallization differentiation seems to terminate, while necks behave as conductors and accumulators of fluid-mobile components.

The late Holocene stage of areal volcanism is characterized by a wide range of concentrations for almost all elements, which is probably due to a combination of different factors: different depths of sources, fluid enrichment, crystallization differentiation, and hybridism of the host rocks (see Figs. 6-V and 7-V). Features of the intraplate geochemical type persist here alongside with island-arc features.

Now we return to a discussion of the Yb–Ce diagram and compare data on the Kekuknai massif with other fluid–magmatic caldera systems (Fig. 8). The rock composition of the Uzon–Geyser-Valley depression and of the Karymskii volcanic center (eastern Kamchatka) and their evolution, which involved the generation of numerous calderas, is significantly different from formations of the Kekuknai volcanic massif, which are similar in dynamics. Moderate-potassium volcanic rocks in the frontal zone of the island arc system show a well-pronounced trend towards

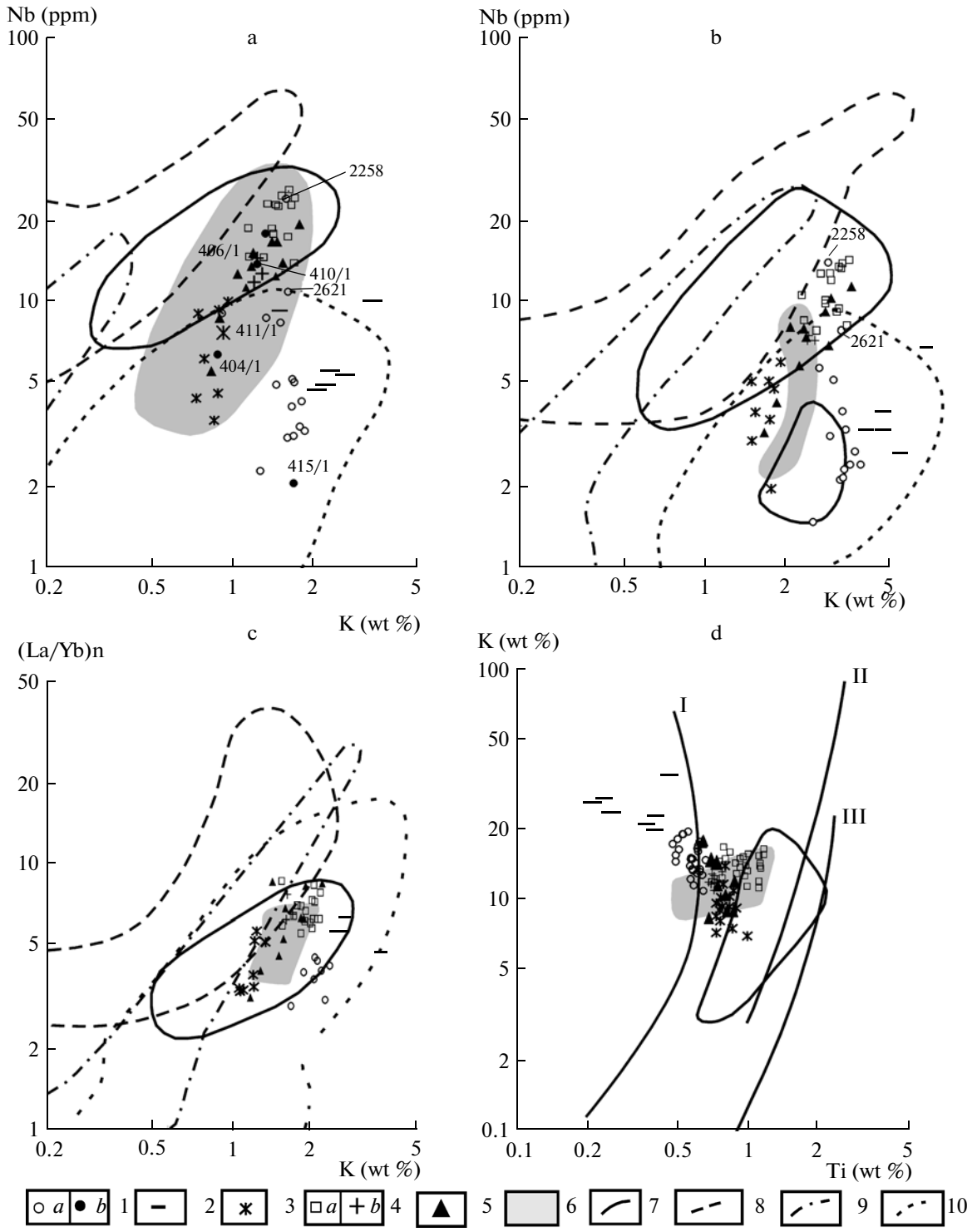

Fig. 4. The Nb–K, Ta–K, $(La/Yb)_n$–K, and K–Ti ratios in rocks of the Kekuknai massif. (1–5) The same as in Fig. 2 (1*a*, data from Table 1, 1*b*, from [Volynets et al., 2010]); (6) field of plateau basalts of intraplate geochemical type in the area of the Ichinskii and Bakening volcanoes. Contours delineate fields: compositions of "Columbia River" basalts (7), Hawaiian volcanic rocks (8), N-MORB (9), island-arc basaltoids (10).

I–III generalized trends of basalt composition evolution: geosynclinal (I), continental riftogenic (II), and oceanic riftogenic (III), after [Lutts, 1980]. For explanations, see the paper. This compilation is based on materials from [Smith, 1992; Hooper and Hawkesworth, 1993; Koloskov, 1999, 2006].

Table 2. Isotopic composition of representative samples from the Kekuknai massif and Mount Khukhch

##	1	2	3	4	5	6	7	8	9	10
Sample no.	pp-2258	pp-2735	415-1*	K-44-05	K-57-05	K-53-05	pp-2614	406-1*	410-1*	pp-2265
Stage	pre-caldera			extrusive	Early stage of areal volcanism		Middle stage of areal volcanism	Late stage of areal volcanism		Mt. Khukhch**
Rock	hawaiite	trachybasalt	trachybasalt	trachyandesite	hawaiite	trachybasalt	hawaiite	hawaiite	hawaiite	basanites
Rb, ppm				42.5	12.8	17.3				
Sr , ppm				512.0	440.0	522.8				
87Rb/86Sr				0.2403	0.0842	0.0957				
87Sr/86Sr	0.703195	0.703227	0.703352	0.703224	0.703284	0.703310	0.703407	0.703106	0.703219	0.703060
Sm, ppm				4.24	4.34	4.08				
Nd, ppm				19.42	18.84	15.30				
$^{147}Sm/^{144}Nd$				0.1319	0.1385	0.1611				
$^{143}Nd/^{144}Nd$	0.513015	0.513095	0.513107	0.513114	0.513044	0.513055	0.513053	0.513036	0.513018	0.513106
$^{206}Pb/^{204}Pb$	18.188	18.177	18.208	18.198	18.114	18.158	18.172	18.112	18.1	18.206
$^{207}Pb/^{204}Pb$	15.488	15.425	15.452	15.457	15.438	15.439	15.476	15.417	15.447	15.461
$^{208}Pb/^{204}Pb$	37.879	37.573	37.724	37.787	37.761	37.724	37.82	37.676	37.808	37.745

Notes: * data from [Volynets et al., 2010];

** Mt. Khukhch subvolcanic body of Pliocene basanites (western Kamchatka), unpublished data by A.B. Perepelov, datings are from [Volynets et al., 2010].

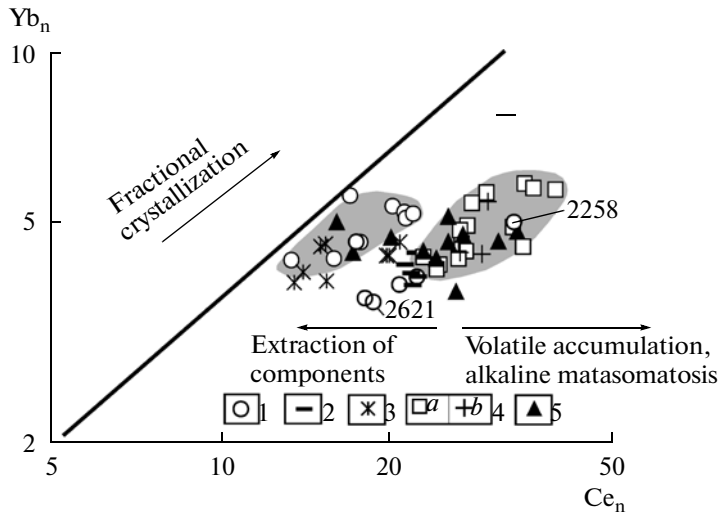

Fig. 5. The Yb_n–Ce_n ratio in rocks of the Kekuknai massif. (1–5) The same as in Fig. 2. The line of fractional crystallization is drawn in accordance with data on Skaergaard rocks [McBirney, 2002]. Element concentrations (ppm) are normalized by their content in pyrolite (primitive mantle) after [Sun and McDonough, 1989]. Fields that show the impact of fractional crystallization are delineated (arrows indicate the direction of supposed change in composition). For explanations, see the paper.

fractional crystallization, whose leading role is stressed by the investigators themselves [Grib et al., 2003, 2009]. The role of the fluid factor is limited here. This attests to the fact that their evolution takes place in the conditions of a closed fluid–magmatic system when "critical accumulation" of volatiles occurs in the residual melt by separation of the crystalline phase. Separate evolution stages of the system differ little, although in the Uzon–Geyser-Valley depression we observe the effect of fluid extraction of components in basaltoids of the post-caldera stage, which nearly disappears when dacites and rhyolites are being generated. For the Karymskii volcanic center the situation is more complex because caldera generation occurred there repeatedly. Compared with these cases, the Kekuknai volcanic massif looks like an open system dominated by fluid dynamics. We observe something like this when analyzing the rock compositions of the "Crater Lake" caldera center in the backarc volcanic basin of the Oregon Plateau [Bacion and Druitt, 1988]. However, alongside intense fluid infusion, traces of fractional crystallization are noted here on a greater scale.

We can now return to the problem of combined island-arc and intraplate geochemical types in the Kekuknai fluid–magmatic system. The classification diagrams (Fig. 4) show that an overwhelming part of the intraplate rocks are situated in fields of the same name determined for regions with a combination of intraplate and island arc geochemical features [Churikova et al., 2001; Dorendorf et al., 2000; Volynets, 1994]. Therefore, the simplest way to explain this peculiarity of Kekuknai volcanic rock composition would be by using the geodynamic and petrologic models developed by the workers referred to above. According to this scenario, the generation of island-arc volcanic rocks during the pre-caldera and extrusive stages might be related to the subduction model, while the intraplate type of areal volcanism might be considered as either some geochemical anomaly resulting from the presence of some additional OIB-type component [Churikova et al., 2001; Dorendorf et al., 2000] in the mantle source or a combination of two mechanisms (subduction of the oceanic plate and the rise mantle diapirs according to the "slab–window" model [Volynets, 1994].

Many features do not agree with these models. As was already mentioned, since the Middle–Late Miocene (8–17 Ma) the volcanism in the western Kamchatka backarc basin should be related to a rifting setting [Perepelov et al., 2007b]. The geological situation of the Kekuknai volcanic massif is in many respects similar to that of the Late Cenozoic volcanism in the backarc basins of North America (Columbia River plateau basalts, Oregon Plateau) [Brandon and Goles, 1998; Carlson and Hart, 1987; Hopper and Hawkesworth, 1993; Smith, 1992]. Taking into account the existing geological situation, we believe that the volcanism in the area of study resulted from incipient backarc rifting with possible involvement (activity) of a mantle plume source, as has been hypothesized for some backarc basins [Brandon and Goles, 1988].

Certainly, we might possibly suppose some alternation of extension and compression regimes in the same region. However, such short periods of reoriented tectonic stresses during relatively short periods of evolution of a single magmatic system seem to be farfetched if they are not supported by other proofs than just the changes in the composition of volcanic rocks.

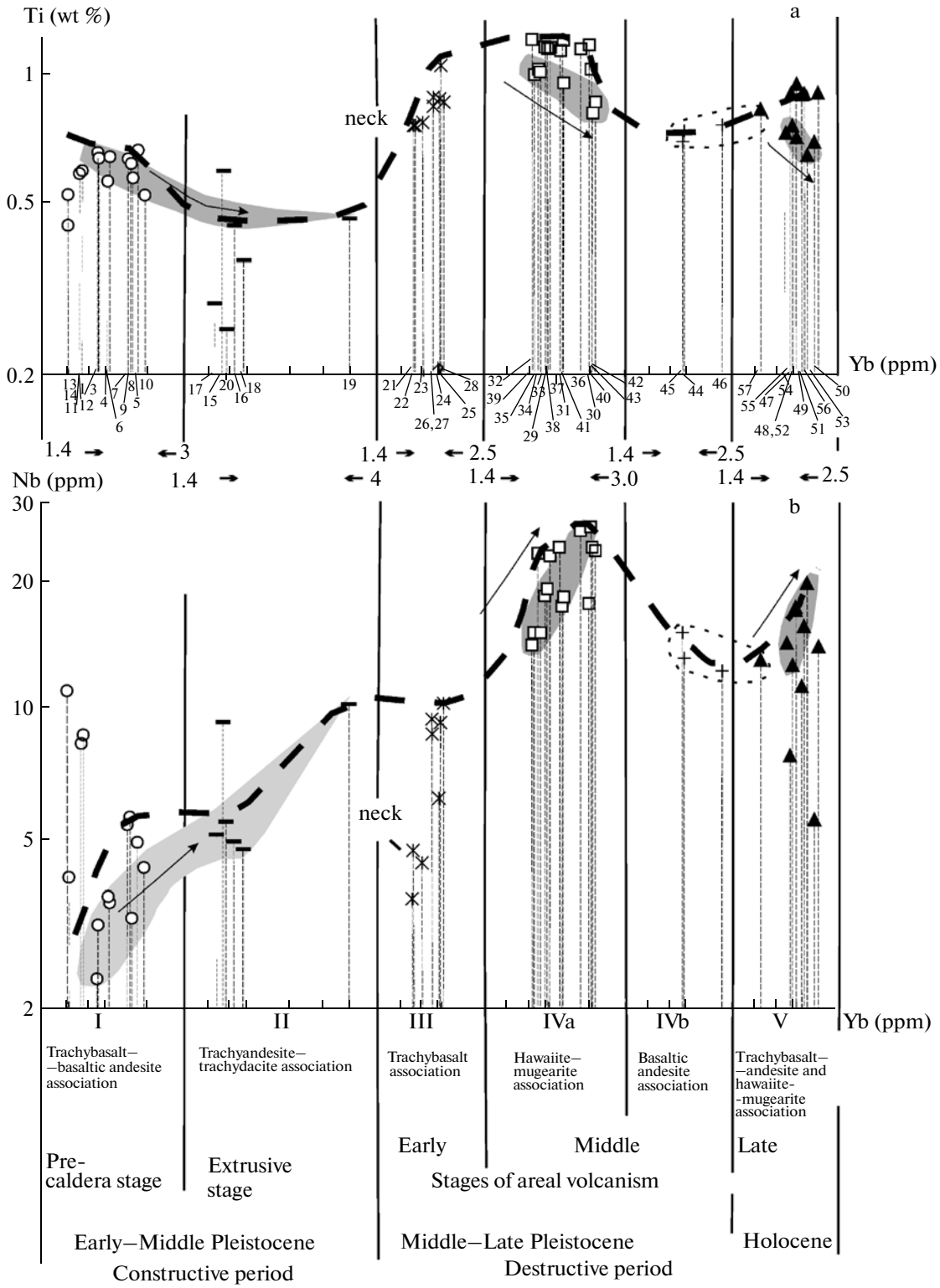

Fig. 6. Generalized diagram of the change of Ti and Nb concentrations in the evolution of melts of the Kekuknai massif. (1–5) The same as in Fig. 2. Element concentrations are plotted against the Yb content in rocks, step-by-step for different stages of the fluid–magmatic system evolution. The identification numbers of the analyses tally with those in Table 1. The filling highlights areas with manifestations of fractional crystallization (arrows indicate the direction of change in composition); the thin dashed lines show localities of possible contamination of melts with crustal material. The extra heavy dashed line denotes the maximum level of accumulation of respective elements. I–V, phases of melt evolution.

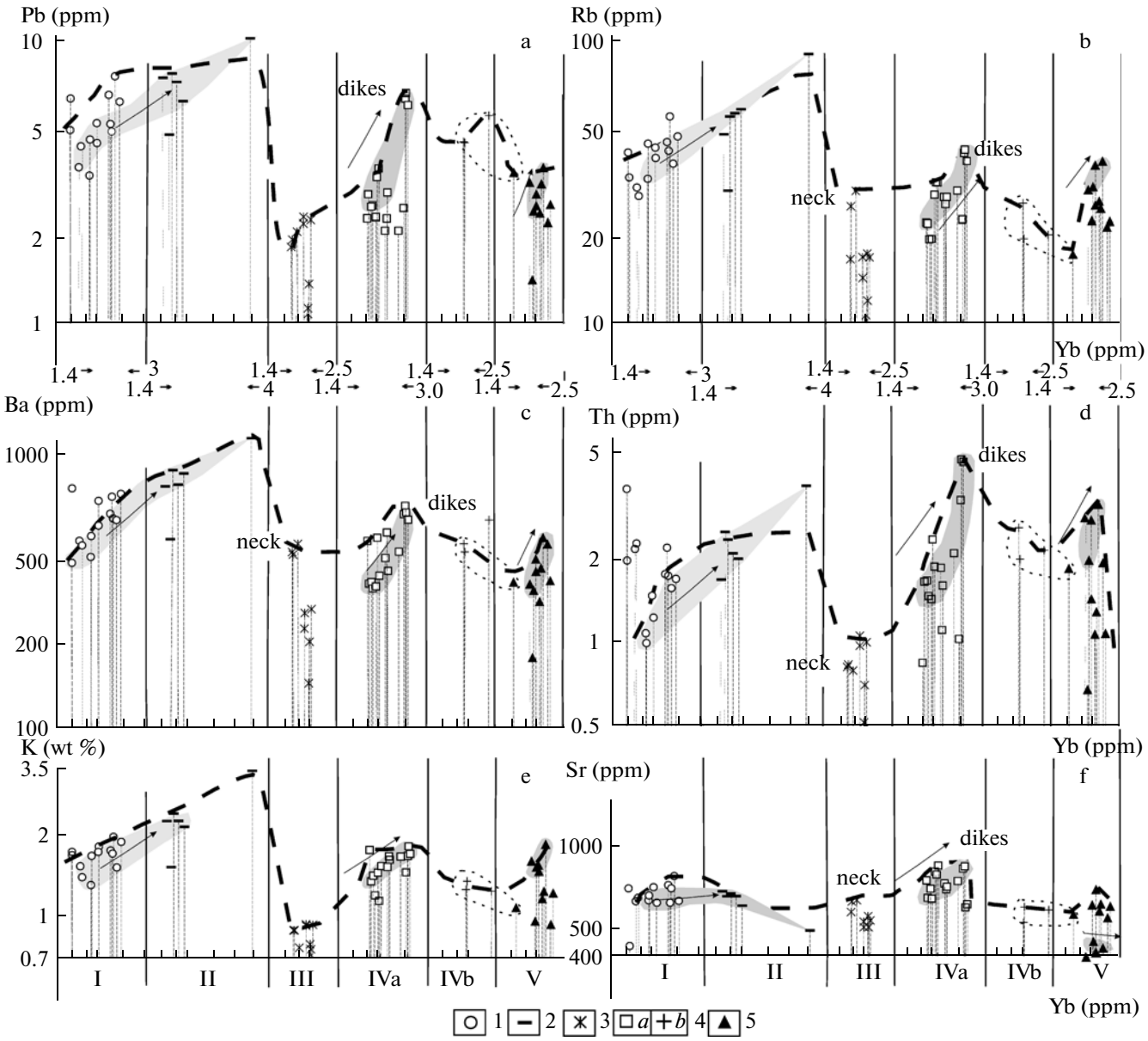

Fig. 7. Generalized diagram of changes in Pb, Rb, Ba, Th, K, and Sr concentrations during evolution of the melts of the Kekuknai massif. The method of construction and the legend are the same as in Fig. 6.

Although the composition of volcanic rocks for the first two stages of the Kekuknai massif evolution in general corresponds to the island-arc geochemical type, some samples with anomalous geochemical compositions were found (Table 1; Figs 4, 8, samples 2258, 2621). Sample 2258 was taken from the plateau at the base of the Bol'shoi Volcano edifice. If the geological setting is not disregarded, the sample should be classified as belonging to the intermediate stage of areal volcanism, based on the evidence of all the other parameters. Sample 2621 was also at the time of sampling identified as belonging to the edifice of Kekuknai Volcano (the pre-caldera stage); it differs from the composition of the associated rocks merely in higher Nb and Ta concentrations and higher silica content. Trachybasalts of the initial stage of areal volcanism (incipient rifting?) possess approximately the same concentrations of high-charge indicator elements (Nb and Ta) as island arc volcanic rocks ("subduction" stage?) and mostly differ from the volcanic rocks of the pre-caldera stage in lower K concentrations (fluid extraction) and higher Ti concentrations (early separation and fractionation of spinels). In addition, compositions intermediate between these two groups are also found (see Figs. 4a and 4b). It is widely believed that high concentrations of fluid-mobile components in an island-arc series largely result from the introduction of volatiles that are released during dehydration of

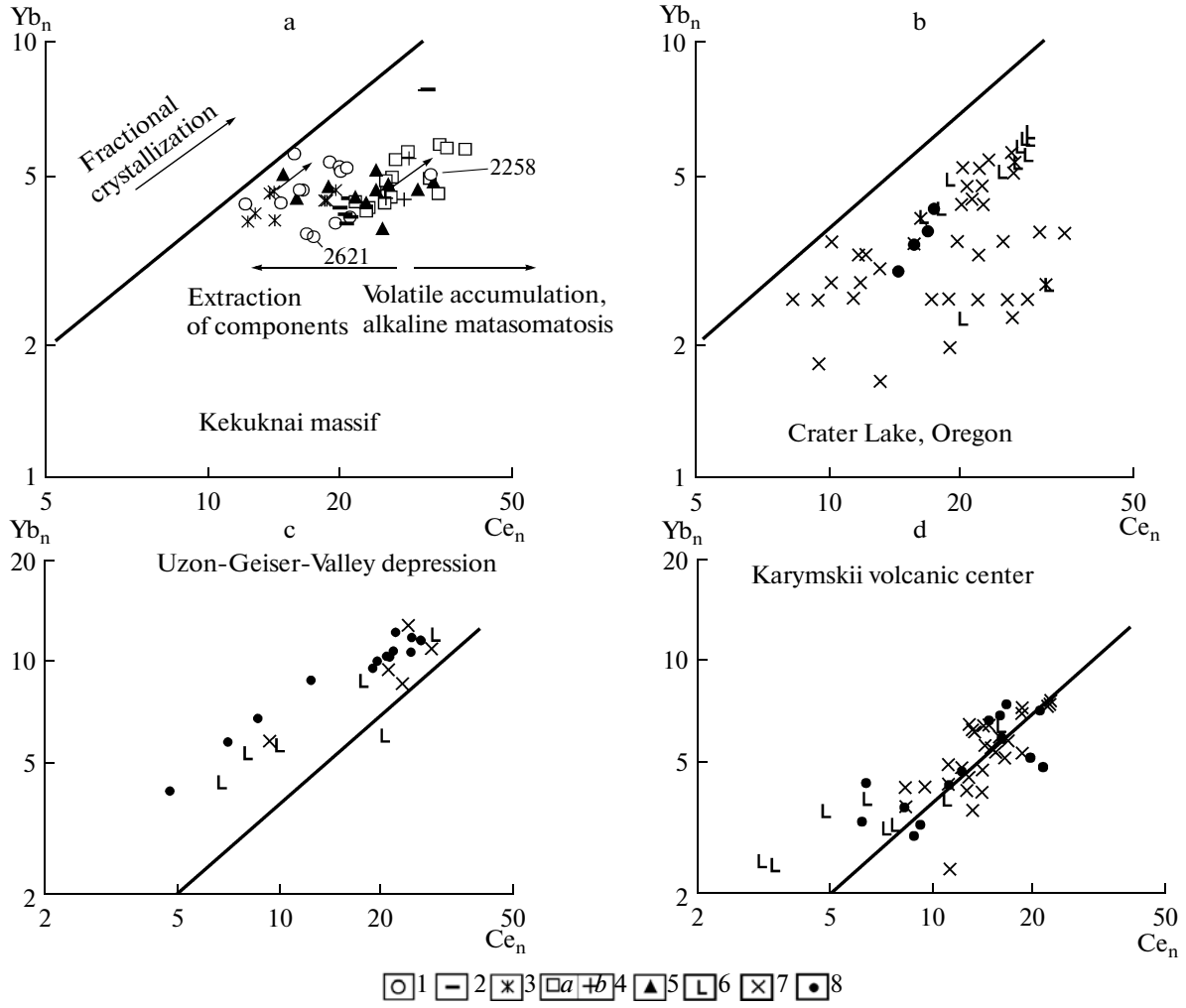

Fig. 8. The Yb_n–Ce_n ratio in the Kekuknai massif rocks and some manifestations of caldera volcanism. (1–5) The same as in Fig. 2; (6–8) rocks of different evolution stages of the fluid–magmatic system: pre-caldera (6), syn-caldera (7), and post-caldera (8). Data from [Bakon and Druitt, 1998; Grib et al., 2003, 2009]. The concentrations of elements in the rocks are normalized by their concentrations in pyrolite (primitive mantle) after [Sun and McDonough, 1989].

the underthrusting oceanic plate (for example, [Pearce, 1983]). Analysis of the Yb–Ce ratio diagram (see Figs. 8c and 8d) demonstrates that this is not always true. In eastern Kamchatka, even in the extreme conditions of caldera generation, the contribution of fluid-mobile components due to dehydration of the underthrusting plate is rather modest and unable to explain the effect of fluidization observed in the Kekuknai fluid–magmatic system. This suggests another conclusion: the subduction mechanism "doesn't work" here. This agrees with the conclusion concerning the absence of a MORB component in the Kekuknai volcanic rocks (see Figs. 4a and 4b) and earlier ideas of other workers that the "main cause of enrichment of effusive high potassium calc–alkaline rocks ... should be sought in the influence of mantle fluids extracting incompatible elements from the surrounding mantle" [Popolitov and Volynets, 1981].

Isotopic analysis is a point that should be dwelt upon. As follows from Table 2, isotopes are pertinent to mantle compositions. Moreover, in the context of overlapping of two isotope systems (Rb–Sr and U–Pb, Fig. 9) the peculiar isotopic composition of the Kekuknai rocks may be thought of as resulting from the mixing of two mantle reservoirs, I and II. The field of enriched mantle reservoir I was identified [Koloskov and Anosov, 2005] as a plume–asthenosphere source when analyzing the isotope characteristics of Kamchatka volcanic rocks by the technique of H. West and W. Leeman [West, Leeman, 1987], which these authors had developed during their study of the "Hawaiian plume." Here, all the figurative points of plateau basalts of the intraplate geochemical type of Kamchatka's Sredinnyi Range (the area of Ichinskii and Bakening volcanoes) occur. In a similar manner, application of the same technique to the data in [Port-

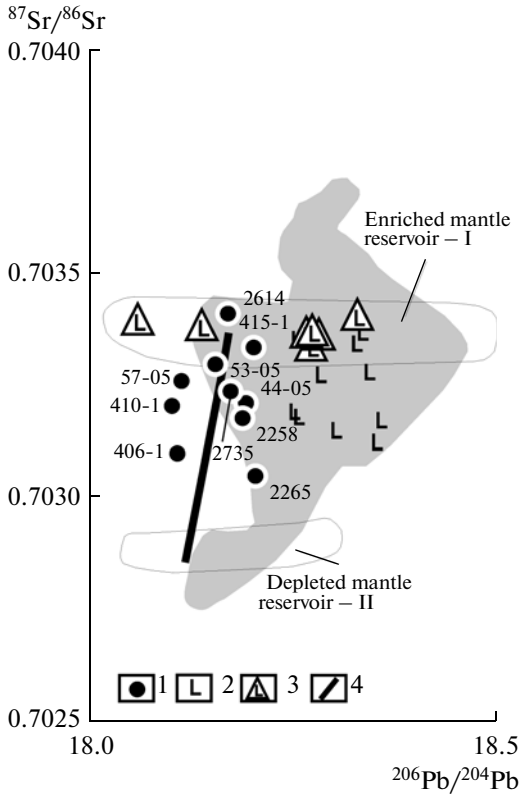

Fig. 9. The $^{87}Sr/^{86}Sr$–$^{206}Pb/^{204}Pb$ ratio in rocks of the Kekuknai massif and the Late Cenozoic volcanic rocks of Kamchatka.

Isotopic compositions: (1) the Kekuknai massif and Neogene basanites of Mount Khukhch. Sample numbers correspond to those in Table 2; (2–3) basalts of the Sredinnyi Range of island-arc (2) and intraplate (3) geochemical types; (4) the trend of supposed shift of original mantle compositions. The darker background highlights the field of the Late Cenozoic volcanic rocks of Kamchatka. For explanations, see the paper. In addition to our own materials, we used data from [Dorendof et al., 2000; Churikova et al., 2001; Portnyagin et al., 2005; Volynets et al., 2010].

nyagin et al., 2005] for Nachiki and Khailyulya volcanoes in eastern Kamchatka identified the depleted mantle reservoir II as a plume–asthenosphere source that characterizes the composition of volcanic rocks in the marginal sea basins of the Asia–Australia region [Koloskov and Fedorov, 2009; Koloskov et al., 2009]. This mantle reservoir could also originate during formation of the Okhotsk Sea basin. As seen in Fig. 9, the points of mantle isotopic compositions from the Kekuknai massif and Mount Khukhch occupy a field of values between fields I and II, which might indicate the combined influence of both sources. Therefore, rocks of the Kekuknai massif involve an enriched mantle component that resulted from the mixing of two Hazaiian-type plume reservoirs. It is characterized by having a high content of potassium (see Figs. 4a and 4b) and other fluid-mobile elements.

As to the geodynamic setting of volcanoes in the region, it is necessary to mention a recent monograph by O.N. Egorov [2009]. This book presents results from a generalization of a vast number of materials on the geology of Miocene–Quaternary volcanic rocks in southeastern Kamchatka within of the centers of endogenous activity identified by this author: Avacha–Ganaly, Banno–Paratunka and Nalacheva, which form the southeastern extension of the backarc volcanic basin under discussion. The author demonstrates that the evolution of these centers occurs via a "common scenario" involving: (1) a stage of active plastic deformation (folding) during Late Oligocene (?)–Miocene time, (2) a stage of cinematic stabilization but activation of upper mantle plumes that were forming Pliocene–Early Pleistocene dome-like uplifts, and (3) a stage of destruction and "taphrogenesis" of these concentric structures in the Middle Pleistocene–Holocene. For the region under discussion, two stages can be defined: a constructive (Pliocene–Early Pleistocene) and a destructive (Middle Pleistocene–Holocene). During the first stage, the dome-like uplift and crowning shield-like volcanic edifices were formed with participation of an upper mantle plume as a source of additional thermal energy and fluid flow. The second stage of initial rifting was marked by destruction of this uplift, appearance of numerous, but unsystematic, variously directed fractures and faults, and manifestation of multivent areal volcanism. The plume source preserved its role, but was at a greater depth and was spatially dispersed.

CONCLUSIONS

1. Five stages of the Kekuknai volcanic massif evolution are defined:

(1) The pre-caldera trachybasalt–andesite basalt, (2) the extrusive trachyandesite–trachydacite, (3) the early trachybasalt, (4) the middle hawaiite–mugearite (with occasional occurrences of basaltic andesites), and (5) the late trachybasalt–hawaiite–mugearite (with occasional occurrences of andesites), with this stage showing areal volcanism. The first two stages are considered as manifestations of the constructive stage and the three subsequent ones as destructive periods in the geological history of the region.

2. Based on geochemical data, island-arc and intraplate geochemical types of rocks are recognized, with some intermediate varieties. The presence of these types in a geological setting unusual for them (a backarc volcanic basin in an island-arc system) indicates convergence of the respective diagnostic features.

3. In general, the rocks of the massif are rich in fluid-mobile elements owing to their formation in an open system, viz., plentiful inflow of fluids occurred with a subordinate role of fractional crystallization and hybridism.

4. The stage of caldera generation involved intense extraction of most fluid-mobile elements (including alkalis) and silica.

5. Formation of the Kekuknai massif occurred in the environment of a backarc volcanic basin under conditions of the commencement of rifting with the active participation of mantle-plume components.

ACKNOWLEDGMENTS

This work was supported by Presidium of the Siberian Branch of the RAS, project IP no. 13 and by the Russian Foundation for Basic Research, project no. 10-10-05-01152-a.

REFERENCES

Antipin, V.S., Volynets, O.N., Perepelov, A.B., et al., Geological Relationships and Geochemical Evolution of the Pliocene–Quaternary Calc–Alkaline and Subalkaline Volcanism of Uksichan Caldera, Kamchatka, in *Geokhimiya magmaticheskikh porod sovremennykh i drevnikh aktivnykh zon* (Geochemistry of Magmatic Rocks of the Present-day and Ancient Active Zones), Tauson, L.V., Ed., Novosibirsk: Nauka, 1987, pp. 73–90.

Bindeman, I.N., Leonov, V.L., Izbekov, P.E., et al., Large-Volume Silicic Volcanism in Kamchatka: Ar–Ar and U–Pb Ages, Isotopic, and Geochemical Characteristics of Major Pre-Holocene Caldera-Forming Eruptions, *J. Volcanol. Geotherm. Res,* 2010, vol. 189, pp. 57–80.

Bacon, C.R. and Druitt, T.H., Compositional Evolution of the Zoned Calc-Alkaline Magma Chamber of Mount Mazama, Crater Lake, Oregon, *Contrib. Mineral. Petrol.,* 1988, vol. 88, pp. 224–256.

Brandon, A.D. and Goles, G.G., A Miocene Subcontinental Plume in the Pacific Northwest: Geochemical Evidence, *Earth. Planet. Sci. Letters,* 1988, vol. 88, pp. 273–283.

Churikova, T.G., Dorendorf, F., and Woerner, G., Sources and Fluids in the Mantle Wedge Below Kamchatka, Evidence from Across-Arc Geochemical Variation, *J. Petrol.*, 2001, vol. 42, no. 8, pp. 1567–1593.

Carlson, R.W. and Hart, W.K., Crustal Genesis on the Oregon Plateau, *J. Geophys. Res.*, 1987, vol. 92, no. B7, pp. 6191–6206.

Dorendorf, F., Churikova, T.G., Koloskov, A.V., and Woerner, G., Late Pleistocene to Holocene Activity at Bakening Volcano and Surrounding Monogenic Centers (Kamchatka): Volcanic Geology and Geochemical Evolution, *J. Volcanol. Geotherm. Res,* 2000, vol. 104, pp. 131–151.

Egorov, O.N., *Strukturoobrazovanie i magmogenez nad verkhnemantiinymi plyumami v vulkanicheskom poyase zony perekhoda okean-kontinent (tsentry endogennoi aktivnosti) (Formation of Structures and Magma Generation above Upper Mantle Plumes in the Volcanic Belt of the Ocean–Continent Transition Zone* (Centers of Endogenous Activity) [electronic resource]: scientific publication, Masurenkov, Yu.P., Ed., Moscow: IFZ Ross. Akad. Nauk, 2009.

Grib, E.N., Perepelov, A.B., and Leonov, V.L., Geochemistry of Volcanic Rocks of Uzon–Geyser-Valley Depression, Kamchatka, *Vulkanol. Seismol.*, 2003, no. 4, pp. 11–28.

Grib, E.N., Leonov, V.L., and Perepelov, A.B., Geochemistry of Volcanic Rocks in the Karymskii Volcanic Center, *Vulkanol. Seismol.*, 2009, no. 6, pp. 3–25.

Hooper, P.R. and Hawkesworth, C.J., Isotopic and Geochemical Constraints on the Origin and Evolution of the Columbia River Basalt, *J. Petrol.*, 1993, vol. 34, no. 6, pp. 1203–1246.

Hart, W.K., Carlson, R.W., Tectonic Controls on Magma Genesis and Evolution in the Northwestern United States, *J. Volcanîl. Geotherm. Res.,* 1987, vol. 32, pp. 119–135.

Klassifikatsiya magmaticheskikh (izverzhennykh) porod i slovar' terminov (Classification of Magmatic (Igneous) Rocks and Dictionary of Terms) Efremova, S.V., Ed., Moscow: Nedra, 1997.

Koloskov, A.V., Flerov, G.B., and Kovalenko, D.V., The Late Cretaceous–Paleocene Magmatic Complexes of Central Kamchatka: Geological Setting and Material Composition, *Tikhookean. Geol.*, 2009, vol. 28, no. 4, pp. 16–34.

Koloskov, A.V., The Koryak–Kamchatka Volcanic Zone, in *Geodinamika, magmatizm i metallogeniya Vostoka Rossii* (Geodynamics, Magmatism, and Metallogeny in Eastern Russia),Book 1,, Khanchuk, A.I., Ed., Vladivostok: Dal'nauka, 2006, pp. 398–417.

Koloskov, A.V., Sr-Isotopic Anomaly in the Kuril Islands: Possible Ways of Explanation, in *Materialy ezhegodnoi konferentsii, posvyashchennoi Dnyu vulkanologa* (Materials of an Annual Conference Devoted to the Volcanologist's Day), Petropavlovsk-Kamchatskii, 2008, pp. 146–153.

Koloskov, A.V., *Ul'traosnovnye vklyucheniya i vulkanity kak samoreguliruyushchayasya geologicheskaya sistema* (Ultrabasic Inclusions and Volcanic Rocks as a Self-Regulated Geological System), Moscow: Nauchnyi Mir, 1999.

Koloskov, A.V. and Anosov, G.I., New Interpretation of Isotope–Geochemical Data for the Pliocene–Quaternary Volcanic Rocks of Kamchatka, in *Materialy ezhegodnoi konferentsii, posvyashchennoi Dnyu vulkanologa* (Materials of an Annual Conference Devoted to the Volcanologist's Day), Petropavlovsk-Kamchatskii, 2005, pp. 7–15.

Koloskov, A.V. and Fedorov, P.I., Basalts of Marginal Basins of Asia–Australia Region in the Context of Concept of Depth Vortical Geodynamics, in *Materialy simpoziuma "Vulkanizm i geodinamika"* (Materials of Symposium "Volcanism and Geodynamics"), Petropavlovsk-Kamchatskii, 2009, pp. 177–180.

Lutts, B.G., *Geokhimiya okeanicheskogo i kontinental'nogo magmatizma* (Geochemistry of Oceanic and Continental Magmatism), Moscow: Nedra, 1980.

Martynov, M.Yu. and Antipin, V.S., Geological and Compositional Evolution of the Uksichan Volcano in the Pliocene and Pleistocene (Sredinnyi Range of Kamchatka), in *Materialy IV Vserossiiskogo simpoziuma po vulkanologii i paleovulkanologii "Vulkanizm i geodinamika" T. 2*, (Materials of the 4th All-Russia Symposium on Volcanology and Paleovolcanology "Volcanism and Geodynamics," vol. 2), Petropavlovsk-Kamchatskii, 2009, pp. 429-432.

McBirney, A.R., The Skaergaard Layered Series. Part VI. Excluded Trace Elements, *J. Petrol.*, 2002, vol. 43, no. 3, pp. 535–556.

Ob"yasnitel'naya zapiska k geologicheskoi karte masshtaba 1 : 200000. List O-57-XXXII. Seriya Zapadno-Kamchatskaya (Explanatory Note to Geological Map at a Scale of 1 : 200000. Sheet O-57-XXXII, Western Kamchatka

Series), Petropavlovsk-Kamchatskii: FGU "KamTFGI", 1986.

Ob"yasnitel'naya zapiska k geologicheskoi karte masshtaba 1 : 200000. List O-57-XXXIII. Seriya Zapadno-Kamchatskaya (Explanatory Note to Geological Map at a Scale of 1: 200000. Sheet O-57-XXXIII, Western Kamchatka Series), Petropavlovsk-Kamchatskii: FGU "KamTFGI", 1992.

Pevzner, M., New Data on Holocene Monogenetic Volcanism of the Northern Kamchatka: Ages and Space Distribution, *Abstr. IVth Int. JKASP Workshop*, 2004, pp. 72–74.

Portnyagin, M., Hoernle, K., Avdeiko, G., et al., Transition from Arc to Oceanic Magmatism at the Kamchatka–Aleutian Junction, *Geology*, 2005, vol. 33, no. 1, pp. 25–28.

Pearce, J.A., Role of the Sub-continental Lithosphere in Magma Genesis at Active Continental Margins, in *Continental Basalts and Mantle Xenoliths*, Hawkesworth, C.J. and Norry, M.J., Eds., Nantwich: Shiva Publ., 1983, pp. 230–249.

Peccerillo, A. and Taylor, S.R., Geochemistry of Eocene Calc-Alkaline Volcanic Rocks from the Kastamonu Area, Northern Turkey, *Contrib. Mineral. Petrol.*, 1976, vol. 58, no. 1, pp. 63–81.

Petrograficheskii kodeks (Petrographic Code) Bogatikov, O.A. et al., Eds., St. Petersburg, 2009, pp. 24–25.

Perepelov, A.B., Puzankov, M.Yu., Ivanov, A.V., et al., Origin of Aenigmatite-Bearing Basaltoids of Parallel Dykes Complex of Western Kamchatka (Magmatism of Late Paleogene Backarc Spreading), in *Probley geokhimii endogennykh protsessov i okruzhayushchei sredy* (Problems of Geochemistry of Endogenous Processes and Environment), Materials of All-Russia Scientific Conference, vol. 2, Irkutsk, 2007a, pp. 176–181.

Perepelov, A.B., Puzankov, M.Yu., Ivanov, A.V., et al., Neogene Basanites of Western Kamchatka: Mineralogical–Geochemical Features and Geodynamic Setting, *Petrologiya*, 2007b, vol. 15, no. 5, pp. 524–546.

Petrologiya i geokhimiya ostrovnykh dug i okrainnykh morei (Petrology and Geochemistry of Island Arcs and Marginal Seas) Bogatikov, O.A., Ed., Moscow: Nauka, 1987.

Popolitov, E.I. and Volynets, O.N., *Geokhimicheskie osobennosti chetvertichnogo vulkanizma Kurilo-Kamchatskoi ostrovnoi dugi i nekotorye voprosy petrogenezisa* (Geochemical Peculiarities of Quaternary Volcanism of Kuril–Kamchatka Island Arc and Some Problems of Petrogenesis), Novosibirsk: Nauka, 1981.

Sun, S.S. and McDonough, W.F., Chemical and Isotopic Systematics of Oceanic Basalts, in *Magmatism in the Ocean Basins, Geol. Soc. Spec. Publ.,* Saunders, A.D. and Norry, M.J., Eds., London, 1989, pp. 313–345.

Smith, A.D., Back-Arc Convection Model for Columbia River Basalt Genesis, *Tectonophysics,* 1992, vol. 207, pp. 269–285.

Volynets, A., Churikova, T., Woerner, G., et al., Mafic Late Miocene–Quaternary Volcanic Rocks in the Kamchatka Back Arc Region: Implications for Subduction Geometry and Slab History at the Pacific–Aleutian Junction, *Contrib. Mineral. Petrol.*, 2010, vol. 159, no. 5, pp. 659–687.

Volynets, O.N., Geochemical Types, Petrology and Genesis of Late Cenozoic Volcanic Rocks from the Kurile-Kamchatka Island Arc System, *International Geological Review*, 1994, vol. 36, no. 4, pp. 373–405.

Vulkany i chetvertichnyi vulkanizm Sredinnogo khrebta Kamchatki (Volcanoes and Quaternary Volcanism of Sredinnyi Range of Kamchatka) Erlikh, E.N., Ed., Moscow: Nauka, 1972.

Volynets, O.N., Koloskov, A.V., Vinogradov, V.I., et al., Isotope Composition of Strontium and Oxygen of the Late Cenozoic K–Na Alkaline Basalts of Intraplate Geochemical Type, Kamchatka, *Petrologiya,* 1995, vol. 3, no. 2, pp. 207–213 [*Petrology* (Engl. Transl.), vol. 3, no. 2, pp.].

Volynets, O.N., Antipin, V.S., Perepelov, A.B., et al., Rare Earths in the Late Cenozoic High-Potassium Volcanic Rocks of Kamchatka, in *Geokhimiya vulkanitov razlichnykh geodinamicheskikh obstanovok* (Geochemistry of Volcanic Rocks of Different Geodynamic Conditions), Tauson, L.V., Ed., Novosibirsk: Nauka, 1986, pp. 149–165.

West, H.B. and Leeman, W.P., Isotopic Evolution of Lavas from Heleakala Crater, Hawaii, *Earth Planet. Sci. Lett.,* 1987, vol. 84, pp. 211–225.

White, R. and McKenzie, D., Magmatism at Rift Zones: The Generation of Volcanic Continental Margins and Flood Basalts, *J. Geophys. Res.,* 1989, vol. 94, no. B6, pp. 7685–7729.

Yasnygina, T.A., Rasskazov, S.V., Markova, M.E., et al., *Opredelenie mikroelementov metodom ISR-MS s primeneniem mikrovolnovogo kislotnogo razlozheniya v vulkanicheskikh porodakh osnovnogo i srednego sostava // Prikladnaya geokhimiya. Analiticheskie issledovaniya. Vyp. 4*, (Trace Element Determination by ICP-MS Method with Application of Microwave Acidic Decomposition in Basic and Intermediate Volcanic Rocks. Applied Geochemistry. Analytical Studies. Issue 4), Burenkov, E.K., Ed., Moscow: IMGRE, 2003, pp. 48–56.